AD-A095 028   HARRY DIAMOND LABS   ADELPHI MD   F/G 19/1
A REVIEW OF MODELS OF THE FLUIDIC GENERATOR.(U)
NOV 80   R DEADWYLER
UNCLASSIFIED   HDL-PR-80-4   NL

1 OF 1
AD A
095028

END
DATE
FILMED
3-81
DTIC

12

HDL-PR-80-4
November 1980

A Review of Models of the Fluidic Generator

by Richard Deadwyler

U.S. Army Electronics Research
and Development Command
Harry Diamond Laboratories
Adelphi, MD 20783

REPORT DOCUMENTATION PAGE		READ INSTRUCTIONS BEFORE COMPLETING FORM
1. REPORT NUMBER HDL-PR-80-4	2. GOVT ACCESSION NO. AD-A095 028	3. RECIPIENT'S CATALOG NUMBER
4. TITLE (*and Subtitle*) A Review of Models of the Fluidic Generator		5. TYPE OF REPORT & PERIOD COVERED Progress Report Sep 1978 to Sep 1979
		6. PERFORMING ORG. REPORT NUMBER
7. AUTHOR(s) Richard Deadwyler		8. CONTRACT OR GRANT NUMBER(s)
9. PERFORMING ORGANIZATION NAME AND ADDRESS Harry Diamond Laboratories 2800 Powder Mill Road Adelphi, MD 20783		10. PROGRAM ELEMENT, PROJECT, TASK AREA & WORK UNIT NUMBERS Program Ele: 63303A
11. CONTROLLING OFFICE NAME AND ADDRESS U.S. Army Materiel Development and Readiness Command Alexandria, VA 22333		12. REPORT DATE November 1980
		13. NUMBER OF PAGES 42
14. MONITORING AGENCY NAME & ADDRESS(*if different from Controlling Office*)		15. SECURITY CLASS. (*of this report*) UNCLASSIFIED
		15a. DECLASSIFICATION DOWNGRADING SCHEDULE

16. DISTRIBUTION STATEMENT (*of this Report*)

Approved for public release; distribution unlimited.

17. DISTRIBUTION STATEMENT (*of the abstract entered in Block 20, if different from Report*)

18. SUPPLEMENTARY NOTES

DRCMS Code: 6433035640012
DA Project: 1X463303D564
PRON: A19EF0070159A9

19. KEY WORDS (*Continue on reverse side if necessary and identify by block number*)

Fluidic generator

20. ABSTRACT (*Continue on reverse side if necessary and identify by block number*)

The fluidic generator is a pneumatic-to-electrical transducer that provides electrical power for the fuze circuits in missiles and rockets. It consists of four subsystems: (1) the jet-forcing mechanism (the annular nozzle and the knife edge of the resonator), (2) the resonant cavity, (3) the mechanical diaphragm assembly (the diaphragm, connecting rod, and reed), and (4) the electrical circuit. The first three subsystems constitute a feedback control

20. ABSTRACT (Cont'd)

system, in which ram-air input to the generator is brought into oscillation with a resonant or reflecting structure controlling the feedback. Pressure feedback signals are generated by sonic reflections from (1) the knife edge, (2) the cavity (assuming that the diaphragm is not moving), and (3) the moving diaphragm. The feedback signals are summed or coupled at the nozzle exit region of the jet. This physical model shows that the generator can be forced to jump to nondesign frequencies of oscillation because any change in the potential of the input jet will change the signal propagation or convection speed in the forward path and the acoustic speed in the feedback path. Thus, the physical model provides a qualitative answer to the question of jumps in the generator operating frequency.

A mathematical model of the complete generator is needed to provide quantitative answers to the question of frequency jumps. Such a model can be developed from the physical model. However, the following generator data are needed to complete the model: annular jet velocity and pressure gain, the signal propagation speed in the forward and feedback paths, and the amplitude path, and summation of the feedback signals.

CONTENTS

Page

FIGURES

FIGURES (Cont'd)

TABLE

1. INTRODUCTION

The fluidic generator[1] shown in figure 1 is a pneumatic-to-electrical transducer which provides electrical power for the fuze circuits in missiles and rockets. In flight, the generator is assumed to operate as follows: air enters the generator via the entrance or inlet port in the nose of the rocket. It exits from the annular nozzle as an annular jet and impinges on the knife edge of the resonant cavity. The cavity has a mechanical diaphragm on the far end. An oscillation is set up in the cavity, which has a frequency and amplitude dependent upon (1) the coupling between the nozzle, the resonant cavity, and the diaphragm; (2) the temperature, pressure, and density of the air in the inlet region; and (3) the geometric parameters of the generator. The ac generator output is rectified by an electrical rectifying circuit so that the generator acts as a dc voltage source.

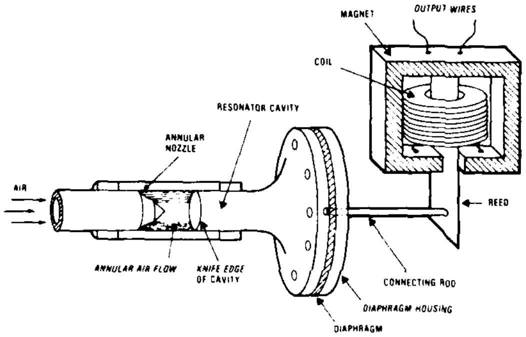

Figure 1. Schematic of fluidic generator (Campagnuolo[1]).

The generator has been designed empirically to meet the requirements for numerous rocket and missile systems. At present, it is used as the power supply for the fuze circuit in the Multiple Launch Rocket System (MLRS). During preliminary testing of the MLRS there were a number of generator failures, which were caused by jumps in the generator operating frequency.* A jump in operating frequency is defined here as a sudden (discontinuous) shift from the nominal or design oscillation frequency to a new frequency and continued oscillation at the new frequency. The jumps in oscillating frequency were eliminated through a redesign of parts of the generator; however, the failures illustrated the need for an in-depth analysis and mathematical model of the complete generator. At present, analyses and mathematical models have been developed only for portions of the generator. A complete mathematical

---

[1] *C. J. Campagnuolo, Some Applications of Fluidics in Fuzing, Harry Diamond Laboratories, HDL-TR-1477 (December 1969).*

**D. W. Finger, Internal Report for Harry Diamond Laboratories, Final Report: Root Cause Analysis, XM445 Fluidic Generator (February 1979).*

model could be used at the design stage to determine whether a given generator can be forced to jump to another operating frequency. It could also be used to optimize generator design and to determine the effect on generator operation caused by parameter changes (parameter changes made to facilitate mass production of the generator).

This is a progress report on the development of a mathematical model of the fluidic generator for the period September 1978 to September 1979. A number of current studies are concerned with testing, designing, and modeling the fluidic generator; however, this report is limited to a review of existing physical and mathematical models of individual portions of the fluidic generator and a synthesis of these models. This report specifically contains a discussion of (1) mathematical modeling, (2) the generator flow field, (3) the generator subsystems, (4) coupling between the subsystems, and (5) a model of the complete generator.

2. MATHEMATICAL MODELING

A mathematical model of a physical system is a mathematical description of the physical phenomena occurring in the system. A useful model therefore requires a thorough analysis or understanding of the physical phenomena involved. This analysis or understanding of the physical phenomena should be such that a "physical model" can be envisioned, which resembles the actual physical phenomena in enough detail to satisfy the given inquiry, but which is simple and thereby more amenable to analytical studies. Therefore, the mathematical model is based on the envisioned physical model. For the fluidic generator shown in figure 1, a physical model requires a thorough analysis of the acoustic-fluid-mechanical-electrical phenomena involved in generator operation. Numerous studies of the fluidic generator have been conducted at the Harry Diamond Laboratories (HDL),[1,2-6] and other agencies; however, the funda-

---

[1] C. J. Campagnuolo, *Some Applications of Fluidics in Fuzing, Harry Diamond Laboratories, HDL-TR-1477 (December 1969)*

[2] C. J. Campagnuolo, *The Fluidic Generator, Harry Diamond Laboratories, HDL-TR-1328 (September 1966).*

[3] C. J. Campagnuolo, *Fluidic Power Generators for Ordance Application, Harry Diamond Laboratories, HDL-TR-1423 (December 1968).*

[4] C. J. Campagnuolo and H. C. Lee, *Review of Some Fluid Oscillators, Harry Diamond Laboratories, HDL-TR-1438 (April 1969).*

[5] H. S. Kimmel, *Development of a Fluidic Velocity Sensor, Harry Diamond Laboratories, HDL-TM-72-6 (March 1972).*

[6] H. C. Lee and C. J. Campagnuolo, *Development of a High Power Wedge-Type Fluidic Generator, Harry Diamond Laboratories, HDL-TM-72-13 (May 1972).*

mental operation has been analyzed in only four studies.[7-9,*] A review of these analytical studies indicates that there has not been a thorough analysis of the complete generator. The studies by Leupold et al[7,8] provide a detailed mathematical model of the magnetic circuit, based on magnetic circuit theory for a circuit with variable magnetic paths. The study by Mitchell[9] provides a detailed model of the internal mechanical components of the generator--that is, the diaphragm, reed, and connecting rod. Finger postulates* a fluidic generator with two basic oscillator mechanisms: the resonant cavity and the diaphragm. Using this theory, a number of in-flight generator failures were duplicated in the laboratory, and the failures were eliminated by redesigning subsequent generators. Nevertheless, a need still exists for a mathematical model of the complete fluidic generator.

3. FLUID FLOW FIELD PRECEDING THE FLUIDIC GENERATOR IN FLIGHT

The fluidic generator shown in figure 2 provides electrical power for rockets and missiles in flight. The fluid input to the system is ram air collected in the nose of the projectile. The MLRS travels at supersonic speed throughout most of its trajectory. The fluid immediately in front of the projectile is also traveling at supersonic speed and, in turn, is preceded by a shock wave. Fine[10] has described the flow field and the shock wave preceding the MLRS in flight. The shock wave preceding the fluidic generator (see fig. 3) in supersonic flight is stationary (not oscillating) relative to the generator so that, given the projectile's trajectory and Mach number, the condition of the air (pressure, temperature, and density) immediately in the rocket (ram air input to the generator) can be determined from Standard Atmospheric Tables[11] and Mach Number Tables.[12]

---

[7] *H. A. Leupold et al, Magnetic Circuit Design Studies for an Inductive Sensor, U.S. Army Electronics Command (ECOM), TR-4158 (October 1973).*

[8] *H. A. Leupold et al, A Flux Circuit Analysis for the Magnetic Transducer of a Fluidic Reed Generator, U.S. Army Electronics Command (ECOM), TR-4284 (January 1975), 2.*

[9] *L. D. Mitchell, Experimental and Theoretical Analysis of a Fluidic Generator, Virginia Polytechnic Institute and State University (in completion of HDL Contract DAAG39-76-R-9164) (August 1977), 4.*

[10] *J. E. Fine, Analysis of Wind Tunnel Test Results of Fluidic Generator for High-Altitude Rocket, Harry Diamond Laboratories, HDL-TR-1877 (March 1979).*

[11] *National Oceanic and Atmospheric Administration, US Standard Atmospheric Tables, Washington, DC (1976).*

[12] *Ames Research Staff, Equations, Tables, and Charts for Compressible Flow, National Advisory Committee for Aeronautics, Report 1135 (1953).*

* *D. W. Finger, Internal Report for Harry Diamond Laboratories, Final Report: Root Cause Analysis, XM445 Fluidic Generator (February 1979).*

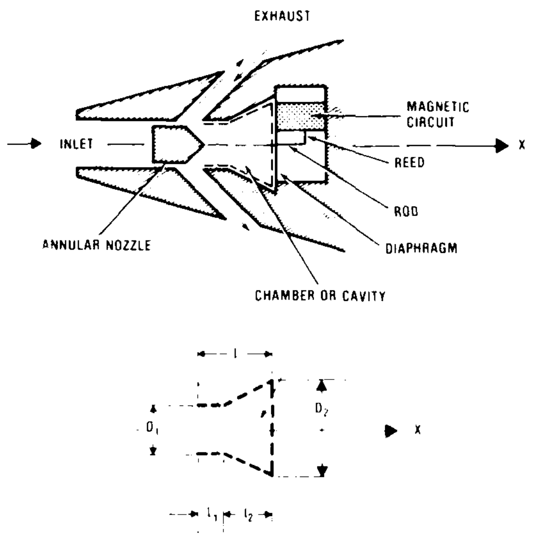

Figure 2. Schematic of fluidic generator in projectile housing (Fine[10]).

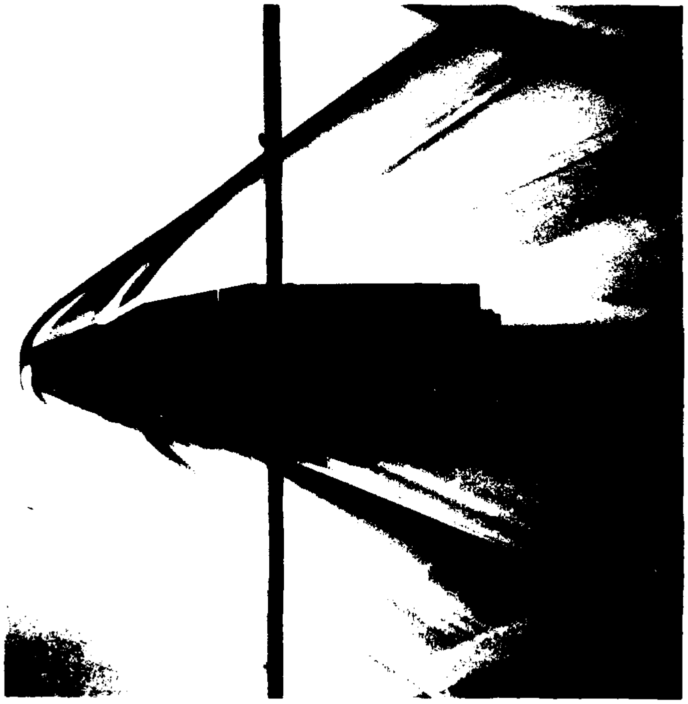

Figure 3. Flow field around multiple launch rocket system projectile in supersonic flight (Fine[10]).

4. PHYSICAL AND MATHEMATICAL MODELS OF THE FLUIDIC GENERATOR SUBSYSTEMS

The fluidic generator can be divided into four separate oscillator subsystems. The four subsystems shown in figure 4 are (1) the jet-forcing system (the annular nozzle and the knife edge of the resonator), (2) the resonant cavity, (3) the mechanical diaphragm assembly (the diaphragm, connecting rod, and reed), and (4) the electrical circuit.

Physical and mathematical models will be postulated for each of the subsystems in the following sections.

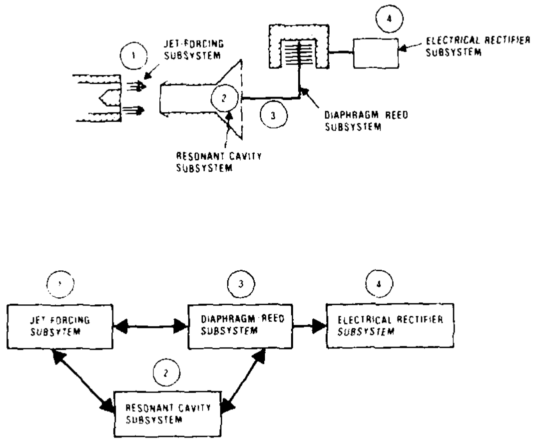

Figure 4. Fluidic generator subsystems.

4.1 Jet-Forcing Subsystem

The jet-forcing subsystem is shown in figure 1. It consists of the inlet region, an annular nozzle, and a sharp-edge, cylindrical ring downstream of the nozzle along the axis. This subsystem has also been described as an acoustic forcing or acoustic triggering mechanism. It has been suggested that the actual physical phenomena involved are either ring-tone oscillation or supersonic screech. Each of these phenomena will be discussed.

Early analyses[9,*] of the generator considered that the forcing phenomena or mechanism was ring-tone oscillation. This type of oscillation is established when fluid pressure developed in the inlet region causes an annular jet to issue from a nozzle and, in the presence of the sharp-edged ring downstream, the annular jet alternately flows into and

---

[9] *L. D. Mitchell, Experimental and Theoretical Analysis of a Fluidic Generator, Virginia Polytechnic Institute and State University (in completion of HDL Contract DAAG39-76-R-9164) (August 1977), 4.*

[*] *D. W. Finger, Internal Report for Harry Diamond Laboratories, Final Report: Root Cause Analysis, XM445 Fluidic Generator (February 1979).*

out of the ring. The fluctuation of the jet creates an audible tone called the ring-tone. The physical phenomena involved--that is, the fluctuation of the jet about the sharp-edged ring--is similar to that in the edge tone and the hole tone shown in figure 5.[13] The edge tone has been studied extensively.[14,15] Most of the analyses are in agreement concerning the following items.

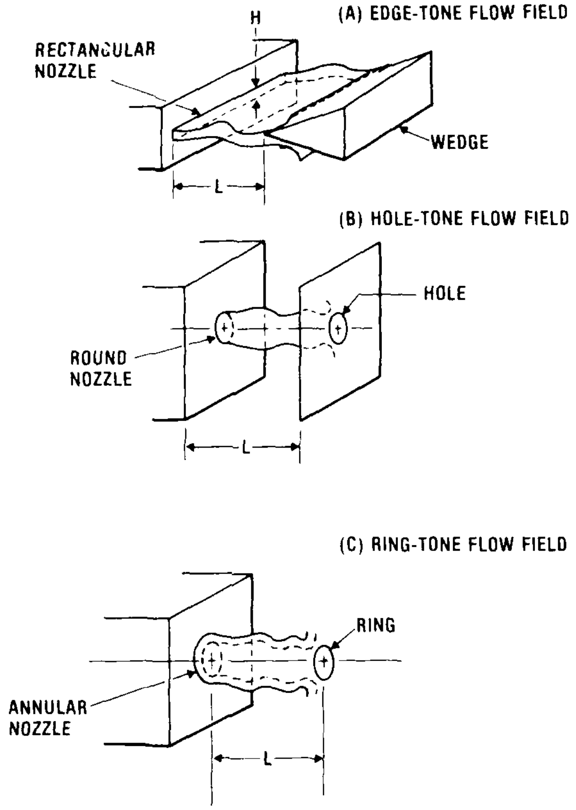

Figure 5. Jet flow patterns for edge-, hole-, and ring-tone oscillations.

---

[13] R. C. Chanaud and A. Powell, *Some Experiments Concerning the Hole and Ring Tone*, J. Acoustic Soc. Am. 37, 5 (May 1965).

[14] G. B. Brown, *The Vortex Motion Causing Edgetones*, Proceedings of the Physical Society (London), 49 (1937), 493.

[15] A. Powell, *On the Edgetone*, J. Acoust. Soc. Am., 33 (April 1961), 395 to 409.

(1) The jet is unstable in the absence of downstream objects (as a function of Reynolds and Strouhal numbers),

(2) The jet is most sensitive to disturbances at the nozzle exit region,

(3) Sinusoidal components of the disturbance (at the nozzle exit region) within the frequency range of jet instability are amplified as they are propagated downstream,

(4) Jet-edge oscillation is a feedback phenomena, and

(5) The feedback pressure signal is generated when the jet strikes the downstream object.

Despite the agreement of various analysts and the study of this phenomena for a long time, the exact physical mechanism of the feedback involved is still not fully understood. Therefore, an encompassing mathematical model describing the mechanism does not exist. Brown[14] gives an empirically derived formula which relates oscillation frequency, nozzle jet velocity, and the distance of the object or sharp edge from the nozzle:

$$f = 0.466j\left[\frac{u - 0.04}{h - 0.0007}\right] , \tag{1}$$

where

f = oscillator frequency (Hz),
u = jet velocity at the nozzle (m/s),
h = distance of the downstream object from the nozzle (m), and
j = a constant, giving the mode of oscillation.

The constant j was experimentally determined to have four values, 1, 2.3, 3.8, and 5.4 corresponding to the first, second, third, and fourth mode or stage of operation. A typical jet-edge frequency versus jet velocity plot with frequency jumps is shown in figure 6. The ring-tone, edge-tone mechanisms are usually associated with low-speed, subsonic jet flow with Reynolds Number < 2000.

The jet-forcing mechanism may also be the supersonic screech phenomena. This phenomena is defined as the audible periodic pressure fluctuations in the far field radiated from a supersonic free jet, which is oscillating due to a feedback phenomena.[16] The jet oscillation and

---

[14] *G. B. Brown, The Vortex Motion Causing Edgetones, Proceedins of the Physical Society (London), 49 (1937), 493.*

[16] *V. Sarohia, Some Flight Simulation Experiments on Jet Noise from Supersonic Underexpanded Flows, AIAH Journal, 16, 7 (July 1978), 710 to 716.*

associated screech tone occur without objects in the flow field. This phenomena can occur in the fluidic generator if the ratio of the nozzle exit pressure to the inlet supply pressure becomes critical (that is, less than or equal to 0.527), so that jet velocity becomes sonic at the nozzle. The mass flow through the annular nozzle is then choked. However, after a distance from the nozzle (dependent on the pressure ratio), the jet expands and then contracts to its original diameter. This process of expansion and contraction repeats itself, being modified or damped only by turbulent mixing. Several cycles can normally be detected by Schlieren photography and form what has been called a cellular pattern (see fig. 7). Shock waves form during the contraction at the end of the cells, growing inwards in the upstream direction from the point of the minimum area so as to finally form a conical structure. Powell[17] describes the mechanism of choked jets and an associated noise in detail. It will be noted here only that the frequency associated with the periodic fluctuations or screech has jumps similar to the edgetone phenomena described earlier.

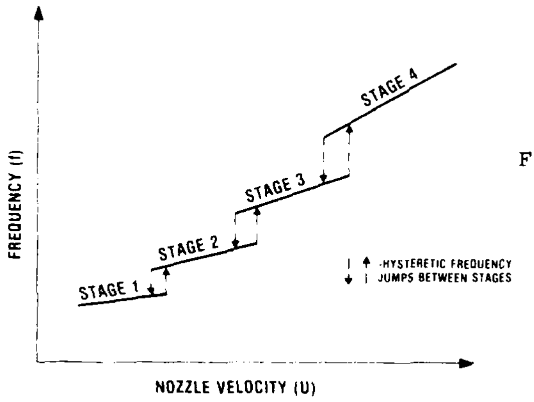

Figure 6. Typical edge-tone frequency versus nozzle velocity plot.

---

[17] A. Powell, *On the Mechanism of Choked Jet Noise, Proceedings of The Physical Society, Ser. B, 66 (1956), 1039 to 1056.*

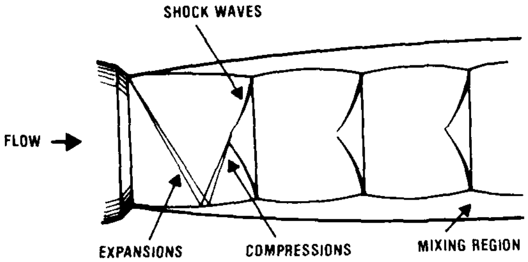

Figure 7. Shock cell structure.

The rise in ram-air temperature due to aerodynamic heating has been postulated as a cause of the frequency jumps observed during MLRS fuze testing.* This rise in air temperature due to aerodynamic heating can be determined by using Standard Atmospheric Tables and Mach Number Tables in the manner used to determine ram-air generator input pressure (see sect. 3). However, if the jet-forcing mechanism is supersonic screech, there will be additional heating of the air if the nozzle-to-cavity opening is such that a compression region of the free jet (fig. 7) exists at the cavity opening. Under these conditions, there will be periodic compression and expansion of the gas within the straight section or neck of the cavity which can cause irreversible temperature increases which are several times the input temperature. This resonance-tube type of heating is described by Sinha.[18] His analysis is of the resonance-tube geometry shown in figure 8. The fluidic generator geometry is somewhat different; however, a resonance-tube type of heating can occur under the conditions described above. Thus, the additional heating which can result from a supersonic screech jet-forcing mechanism is another reason for determining which of the two phenomena is involved. The actual forcing mechanism involved in the fluidic generator, whether ring-tone or supersonic screech, can be determined by measuring the nozzle exit velocity.

4.2 Resonant Cavity Subsystem

The resonant cavity subsystem of the fluidic generator consists of the fixed volume outlined by the dashed line in figure 2. This portion of the system is normally thought of as a passive acoustic or fluidic resonant circuit with high Q (narrow bandpass). It has been modeled as a closed organ pipe and as a Helmholtz resonator. If the

---

[18] *R. Sinha, A Theoretical Analysis of Resonance Tube, The Singer Company Kearfott Division, Final Report KD 72-82, for Department of the Army, Picatinny Arsenal, Contract No. DAAA 21-72-C-0500 (October 1972).*

**D. W. Finger, Internal Report for Harry Diamond Laboratories, Final Report: Root Cause Analysis, XM445 Fluidic Generator (February 1979).*

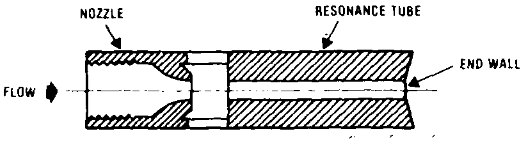

Figure 8. Schematic diagram--resonance-tube configuration (Sinha[18]).

cavity is thought of as a closed organ pipe, then physically the acoustic disturbance at the mouth of the cavity must be a plane wave and propagate through the cavity in the x direction only along the primary axis of the cavity (see fig. 2). This physical model neglects the enlarged volume of the truncated cone section of the cavity. The mathematical model for this closed pipe gives a resonant frequency, f, of

$$f = \frac{(N - 1/2)c}{2(\ell)} , \qquad (2)$$

where ℓ = the length of the cavity (m),
c = the speed of sound in the cavity (m/s), and
$N = 1,2,3...$

Modeling the cavity in this manner also implies that harmonics $N = 2, 3...$ are important.

If the cavity is thought of as a Helmholtz resonator, then physically the acoustic disturbance at the mouth of the cavity causes the air in the neck or straight section (fig. 2) to move as a unit (or as a mass element). The air within the truncated cone section of the cavity acts as a pneumatic spring as it is alternately compressed and expanded by the mass element at the resonant frequency. The instantaneous pressure is the same throughout the truncated cone section of the cavity. When the cavity is modeled as a Helmholtz oscillator, it has an electrical equivalent circuit impedance to acoustic or fluidic input like that shown in figure 9, where pressure is the variable analogous to voltage, and volume flow is the variable analogous to current. A lumped-parameter model can be used when the wave number, λ, which is equal to $k_\omega/2\pi$, is large with respect to the largest cavity dimension. The equivalent resistance accounts for any signal loss in the cavity due to frictional heating or radiation. The process is thought to be isothermal; therefore, the resistive losses are due to radiation. Resistance, R, is given as

$$R_p = \frac{\rho c k_\omega^2}{2\pi^2} , \qquad (3)$$

where ρ = fluid density, (kg/m^3),
c = speed of sound in the medium, $\sqrt{n \frac{P_{avg}}{\rho}}$ (m/s),

n = polytropic constant,
k_ω = wavelength constant $\frac{\omega}{c}$ (1/m), and
ω = $2\pi f$ = angular frequency (rad/s).

The inertance, L_p, accounts for the tendency of the air in the neck or straight section of the cavity to move as a solid mass or slug of air. It is given as

$$L_p = \frac{4\rho\ \ell_1}{\pi D_1^2} \quad , \tag{4}$$

where ℓ_1 = length of the straight section (m),
ρ = fluid density (kg/m^3), and
D_1 = diameter of the straight section (m).

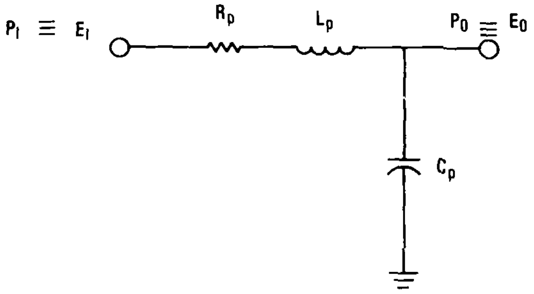

Figure 9. Electrical equivalent circuit for Helmholtz resonator.

The equivalent capacitance describes the compressibility of the air in the truncated cone section of the cavity. It is given as

$$C_p = \frac{V}{nP_{avg}} = \frac{\frac{\pi}{4}\ \ell_2\left[\frac{1}{3}\left(D_2 - D_1\right)^2 + D_1\left(D_2 - D_1\right) + D_1^2\right]}{nP_{avg}} \tag{5}$$

where V = volume of the truncated cone section of the cavity (m^3),
ℓ_2 = length of the truncated cone section (m),
D_2 = large diameter of truncated cone (m), and
P_{avg} = average pressure in the truncated cone section of the cavity (N/m^2).

The transfer function for the equivalent circuit is

$$\frac{P_O}{P_I} = \frac{1}{L_p C_p s^2 + R_p C_p s^2 + 1} \quad . \tag{6}$$

Thus, the resonant frequency is

$$f = \frac{1}{2\pi}\sqrt{\frac{1}{L_pC_p}} = \frac{1}{2\pi}\sqrt{\frac{nP_{avg}D_1^2}{\rho\ell_1\ell_2\left[\frac{1}{3}\left(D_2 - D_1\right)^2 + D_1\left(D_2 - D_1\right) + D_1^2\right]}} \qquad (7)$$

The frequency given by the Helmholtz resonater model of the cavity corresponds to the fundamental resonant mode of oscillation given by the organ pipe model equation (2), where N = 1.

Finally, the cavity can be described as a mechanical waveguide, as discussed by Schmidlin[19] and Franke et al.[20] This model was based on a solution of the wave equation treating the cavity as a mechanical waveguide. The initial analysis by Schmidlin[19] of the cylindrical cavity showed a series of resonant frequencies which were functions of the cavity dimensions and the acoustic speed in the fluid. Subsequent experiments by Franke[20] verified the analytical results.

4.3 Mechanical Diaphragm Subsystem

The mechanical diaphragm assembly or subsystem consists of the diaphragm, connecting rod, reed, and the connecting hardware shown in figure 1. The study by Mitchell[9] gives a thorough physical and mathematical description of this subsystem. The mechanical impedance circuit model of the subsystem is shown in figure 10. A digital computer, mechanical circuit-analysis program called the Impedance Modeling Program (IMP, version V)[21] was used to analyze the mathematical model of the diaphragm assembly and to predict the response of the reed to a dynamic input pressure on the diaphragm. It should be noted that this model of the diaphragm accounts for only the first natural mode of oscillation of the diaphragm. The theoretical response compares well with dynamic test data on the subsystem (see fig. 11).

---

[9] *L. D. Mitchell, Experimental and Theoretical Analysis of a Fluidic Generator, Virginia Polytechnic Institute and State University (in completion of HDL Contract DAAG39-76-R-9164) (August 1977), 4.*

[19] *A. E. Schmidlin and E. L. Rakowsky, A Jet Driven Flueric Oscillator, Advances in Fluidics, ASME (1967), 282 to 297.*

[20] *M. E. Franke, G. Jones, III, and H. A. Olsen, Jet Driven Cylindrical Cavity Oscillators, ASME Paper No. 72-WA/Flcs-4 (November 1972).*

[21] *L. D. Mitchell, Program Documentation: IMPV Class Notes for ME 5120, available from the Department of Mechanical Engineering, Randolph Hall, Virginia Polytechnic Institute and State University, Blacksburg, VA (n.d.).*

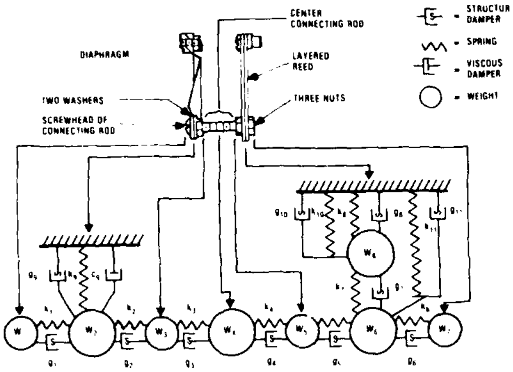

Figure 10. Mechanical equivalent lumped-parameter network of fluidic generator diaphragm, connecting rod, and reed subsystem (Mitchell[9]).

Figure 11. Theoretical and experimental dynamic compliance of the fluidic generator diaphragm/ reed subsystem (Mitchell[9]).

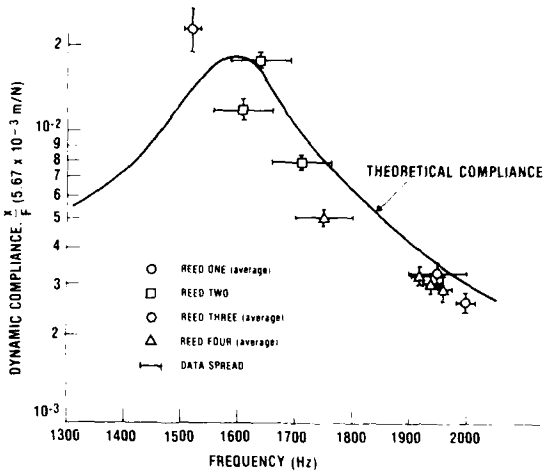

The electrical equivalent circuit model of the diaphragm is shown in figure 12, where force is the variable analogous to voltage, and velocity is the variable analogous to current. This is a very detailed circuit model; it can be simplified by assuming that the center of the diaphragm, connecting rod and end of the reed move as a single body. This simplification leads to the circuit in figure 13. The simplified electrical equivalent circuit model is shown in figure 14. This network is still rather complicated, and it is useful to analyze it with an electric circuit-analysis program. The electrical equivalent inductance L_m accounts for the masses in the system:

$$L_m = \frac{m}{A_D^2} , \qquad (8)$$

where A_D = area of the diaphragm (m^2) and
m = mass (kg).

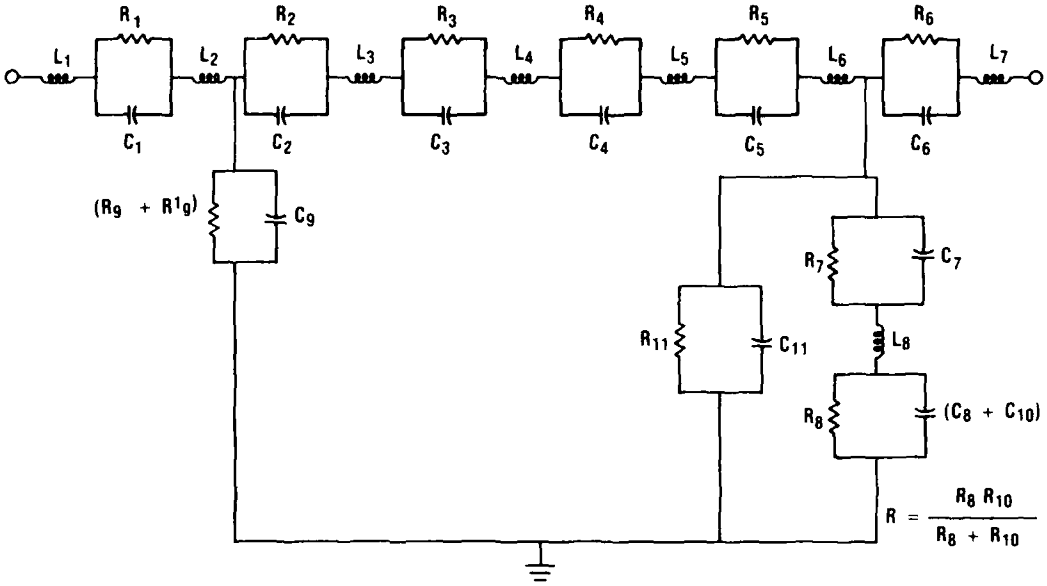

Figure 12. Electrical equivalent of mechanical network shown in figure 10.

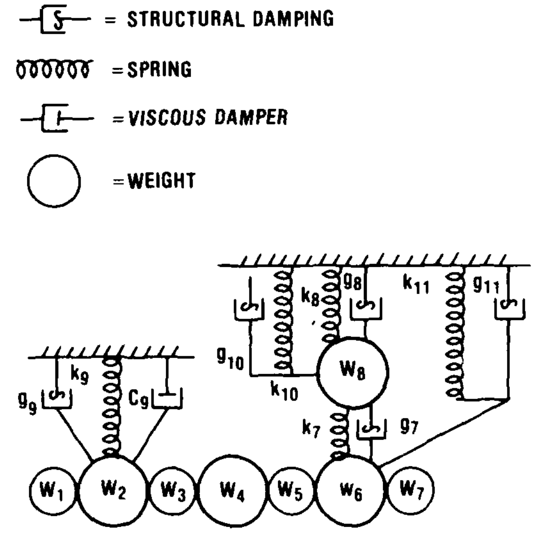

Figure 13. Simplified version of mechanical network shown in figure 10.

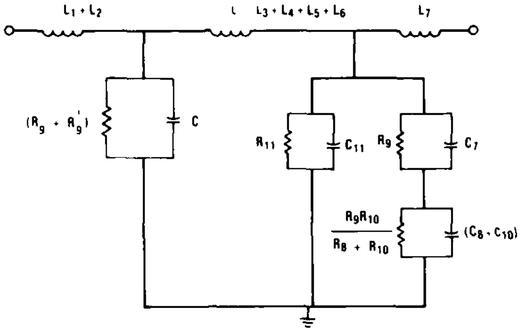

Figure 14. Electrical equivalent of mechanical network shown in figure 13.

The electrical equivalent capacitance, C_m, accounts for the compliances in the system. It is given as

$$C_m = \frac{A_D^2}{k} \quad , \tag{9}$$

where

k = mechanical spring rate of compliances in the system (N/m).

The equivalent resistance R accounts for the structural and viscous damping in the system. It is given as

$$R_m = \frac{g}{A_D^2} \quad , \tag{10}$$

where g = mass rate (kg/s).

4.4 Electrical Subsystems

The electrical subsystem of the fluidic generator consists of the coil in the magnetic field (see fig. 15), and the fuze circuit load. The coil impedance, Z_c, is

$$Z_c\ (s) = R_c + sL_c \quad , \tag{11}$$

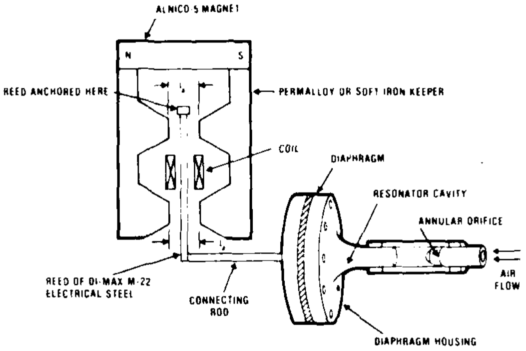

Figure 15. Schematic view of fluidic generator with reed-type magnetic transducer (Leupold et al[8]).

where R_c is the coil resistance and L_c is the inductance of the coil which varies as a function of the reed's position in the air gap of the magnetic circuit. The electronic fuze circuit shown in figure 16 actually is not a part of the fluidic generator. The fuze circuit is the generator load. However, it is reactive so that the generator output voltage is a function of fuze circuit impedance. Therefore, for this analysis it is considered part of the electrical subsystem of the generator.

Capacitor C_1 (fig. 16), in series with the coil circuit impedance, is used to provide an electrical series resonant circuit, which is close to the resonant frequency of the first three subsystems. This electrical series resonance boosts the output voltage of the generator when the MLRS is at high altitude. The fluidic generator ac output voltage is measured across terminals B and G in figure 16. The R_{113}, R_{116}, C_{107} circuit is used for compatibility with the telemetry (TM) instrumentation.

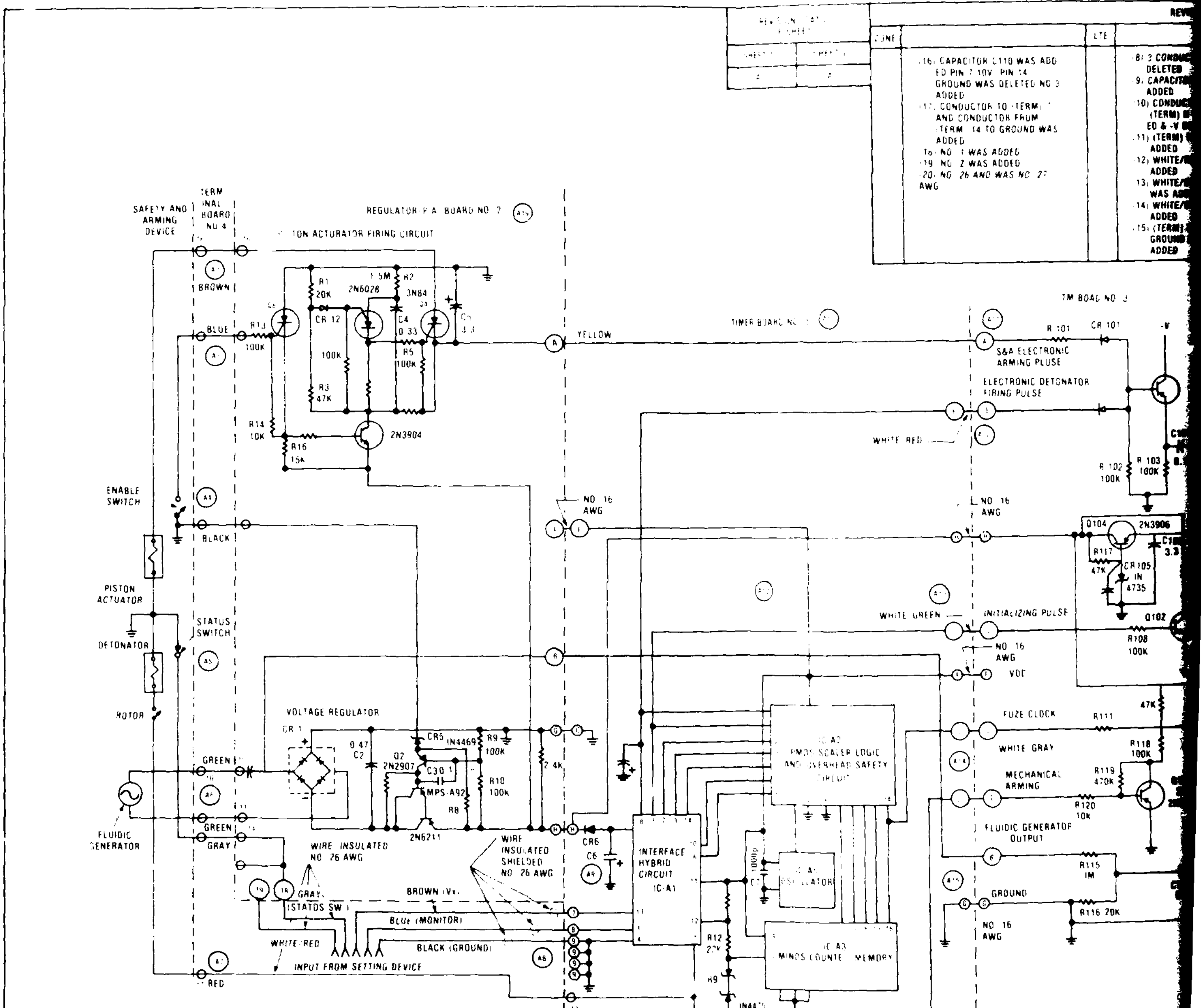

NOTES

1 USAS Y 32 2 APPLIES
2 ALL RESISTORS 1 8 W UNLESS OTHERWISE NOTED
3 ALL CAPACITORS IN F UNLESS OTHERWISE NOTED
4 ALL ELECTRICAL INTERFACES TO SETTING DEVICE AND TELEMETRY 26 AWG STRANDED TEFLON INSULATION
5 STATUS SWITCH CLOSED UNTIL MECHANICAL ARMING
6 ODFNOTES P C PADS
7 UNLESS OTHERWISE NOTED ALL INTERCONNECTING WIRES ARE NO 26 AWG (A20)

Figure 16. XM445 fuze, electronic schematic diagram.

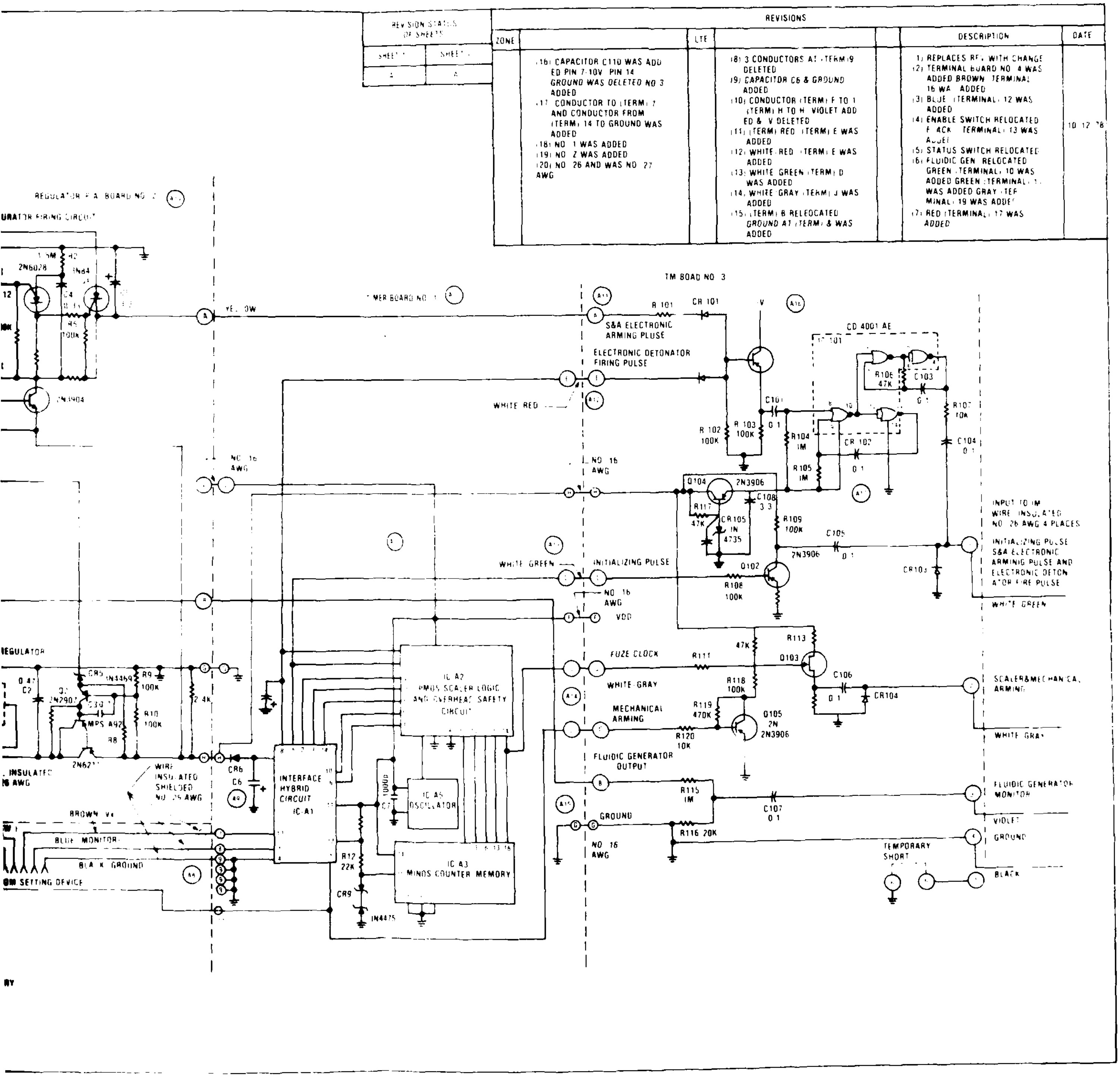

REVISION STATUS OF SHEETS	
SHEET	SHEET
A	A

ZONE	REVISIONS	LTE			DESCRIPTION	DATE
	(16) CAPACITOR C110 WAS ADDED PIN 7-10V PIN 14 *GROUND WAS DELETED NO 3* ADDED (17) CONDUCTOR TO (TERM) 7 AND CONDUCTOR FROM (TERM) 14 TO GROUND WAS ADDED (18) NO 1 WAS ADDED (19) NO Z WAS ADDED (20) NO 26 AND WAS NO 27 AWG		(8) 3 CONDUCTORS AT (TERM) 9 DELETED (9) *CAPACITOR C6 & GROUND* ADDED (10) CONDUCTOR (TERM) F TO 1 (TERM) H TO H VIOLET ADDED & V DELETED (11) (TERM) RED (TERM) E WAS ADDED (12) WHITE RED (TERM) E WAS ADDED (13) WHITE GREEN (TERM) D WAS ADDED (14) WHITE GRAY (TERM) J WAS ADDED (15) (TERM) B RELEOCATED *GROUND AT (TERM) & WAS* ADDED		1) REPLACES REV WITH CHANGE (2) TERMINAL BOARD NO 4 WAS ADDED BROWN TERMINAL 16 WA ADDED (3) BLUE (TERMINAL) 12 WAS ADDED (4) ENABLE SWITCH RELOCATED F ACK TERMINAL) 13 WAS ADDED (5) STATUS SWITCH RELOCATED (6) FLUIDIC GEN RELOCATED GREEN (TERMINAL) 10 WAS ADDED GREEN (TERMINAL) WAS ADDED GRAY (TERMINAL) 19 WAS ADDED (7) RED (TERMINAL) 17 WAS *ADDED*	10 12 78

Figure 16. XM445 fuze, electronic schematic diagram.

5. COUPLING BETWEEN THE OSCILLATOR SUBSYSTEMS

The coupling between the subsystems described in section 4 will now be discussed.

5.1 Jet-Forcing, Resonant-Cavity Coupling

The jet-forcing, resonant-cavity coupling can take the form of ring-tone, resonant-cavity coupling or supersonic screech-resonant cavity coupling. In either case, this is a Class-III oscillator system as discussed by Chanaud.[22] In a Class-III system, a steady stream of air is brought into oscillation with a resonant or reflecting structure controlling the feedback. Ring-tone resonant-cavity couping will be considered first. This coupling is complicated by a lack of details about the ring-tone feedback mechanism, as discussed in section 4.1. However, this type of coupled mode oscillator system has been studied by several authors. These studies have concerned resonant cavities of various shapes and various jet orientations to the plane of the mouth of the cavity. However, they are all coupled-mode oscillator systems. The study by Campagnuolo* concerned the single-sided rectangular cavity shown in figure 17, where the jet flow is parallel to the mouth of the cavity. Campagnuolo* considered many variations in cavity geometry and nozzle jet velocity. He was able to correlate the data generated by these parameter variations and obtain an empirical equation which gives the approximate system frequency. Gaylord's study[23] was concerned with the doubled-sided or dual-rectangular cavity geometry shown in figure 18. Here again the jet flow is parallel to the mouth of the cavities. Gaylord[23] varied cavity geometry in order to increase the amplitude of oscillation in the cavity. He also obtained an empirical equation which gives the approximate frequency of oscillation. Kirshner† used a control volume technique to derive an equation for the jet-edge resonant-cavity coupling frequencies (fig. 19) (this oscillation mechanism is similar to that for the ring tone). His work essentially involved double-sided rectangular cavities similar to the one described by

---

[22] *R. C. Chanaud, Aerodynamic Whistles, Scientific American, 222, 1 (January 1970), 40 to 46.*

[23] *W. Gaylord and V. Carter, Flueric Temperature-Sensing Oscillator Design, Harry Diamond Laboratories, HDL-TR-1428 (April 1969).*

**C. J. Campagnuolo, Experimental Analysis of Self-Maintained Oscillations of a Jet-Edge System with a Resonating Cavity, Master's thesis, Georgetown University (1962).*

†Personal Communication with Mr. J. M. Kirshner, former Chief of the Fluidics Research Branch, Harry Diamond Laboratories, January 1979.

Gaylord.[23] Franke et al[20] considered the jet-driven cylindrical cavity oscillator shown in figure 20. The cavity is driven by an air jet that enters the cavity radially through a nozzle on the periphery of the cavity. The operating frequencies of the oscillator were found to agree with the eigenfrequencies of the cavity; however, the regions of operation at these frequencies were shown to depend on the flow rate and to exhibit characteristics similar to those of a multistage jet-edge resonator. Morel's work[24] involved a round jet used to drive a coaxial cylindrical cavity with an exhaust port (see fig. 21). He was able to derive an equation for the coupling frequencies, that is, the frequencies at which the hole tone (the oscillator mechanism is the same as that for the ring tone) and the cavity are coupled to produce a strong single-frequency oscillation. The studies by these authors are summarized in table 1. In these studies, frequency jumps were observed or theorized in every case, and the cause in each case was increasing jet velocity.

A coupled supersonic-screech, resonant-cavity system operates similarly to the ring-tone resonant-cavity system. They are similar in that the ring-tone and supersonic-screech tone employ an unstable jet, amplify disturbance near the nozzle, are geometrically similar, and are feedback mechanisms. The big difference is in flow rate. In supersonic screech systems, the mass flow (or jet velocity) in the nozzle is choked or sonic. However, not all aspects of supersonic Class-III whistles[22] are understood. The use of a Galton whistle (fig. 22) by Rice[25] as a sonic altimeter for aircraft is an example of a supersonic-screech, resonant-cavity system. The flow in the nozzle is choked or sonic; however, the underexpanded jet expands and becomes supersonic as it leaves the nozzle. Information obtained from the study by Rice[25] is also given in table 1. The question of frequency jumps was not addressed.

Information on the HDL fluidic generator and Class-III whistles[22] or resonator systems is also given in table 1 so that comparisons can be made. It should be noted that the cavity configurations listed in table 1, with the exception of the fluidic generator, are rigid and do not have moving sections (such as the diaphragm in the fluidic generator).

---

[20] *M. E. Franke, G. Jones, III, and H. A. Olsen, Jet Driven Cylindrical Cavity Oscillators, ASME Paper No. 72-WA/Flcs-4 (November 1972).*

[22] *R. C. Chanand, Aerodynamic Whistles, Scientific American, 222, 1 (January 1970), 40 to 46.*

[23] *W. Gaylord and V. Carter, Flueric Temperature-Sensing Oscillator Design, Harry Diamond Laboratories, HDL-TR-1428 (April 1969).*

[24] *T. Morel, Experimental Study of a Jet-Driven Helmholtz Oscillator, ASME Winter Annual Meeting, San Francisco, CA (December 1978).*

[25] *C. W. Rice, Sonic Altimeter for Aircraft, Aeronautical Engineer (Trans. ASME), 4 (1932), 61 to 76.*

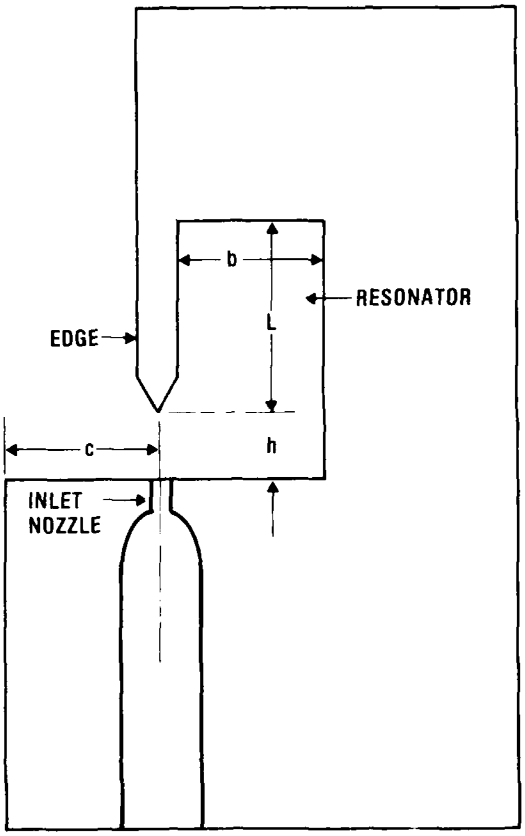

Figure 17. Schematic of single-cavity jet-edge resonator oscillator (C. J. Campagnuolo, Master's thesis, Georgetown University, 1962).

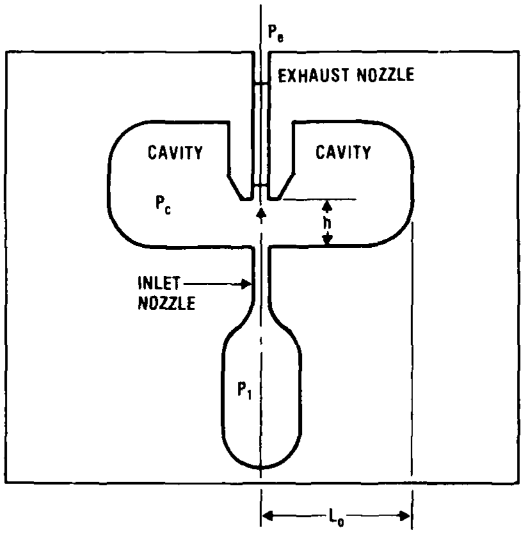

Figure 18. Schematic of double-cavity jet-edge resonator oscillator (Gaylord and Carter[23]).

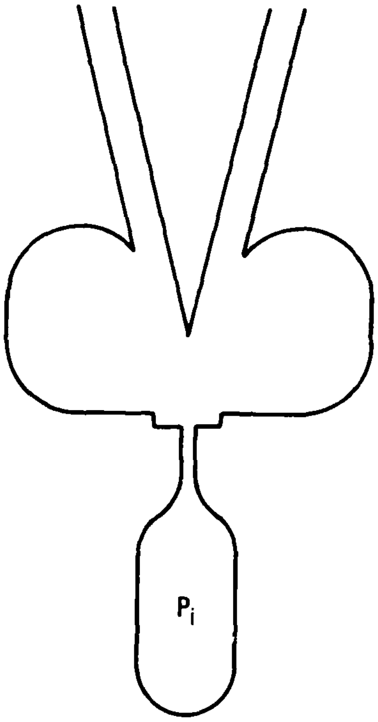

Figure 19. Schematic of edge-tone cavity oscillator.

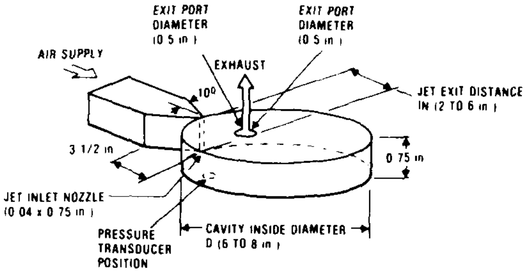

Figure 20. Schematic of cylindrical cavity oscillator (Franke et al[20]).

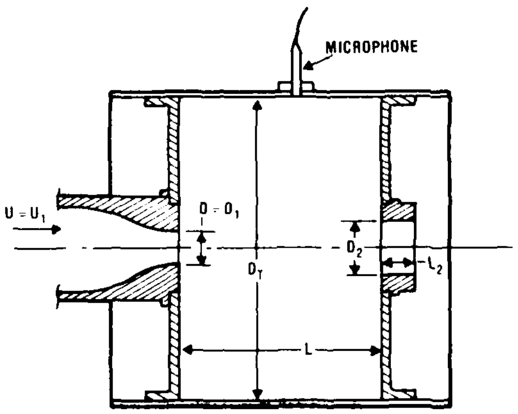

Figure 21. Schematic of jet-driven Helmholtz oscillator (Morel[24]).

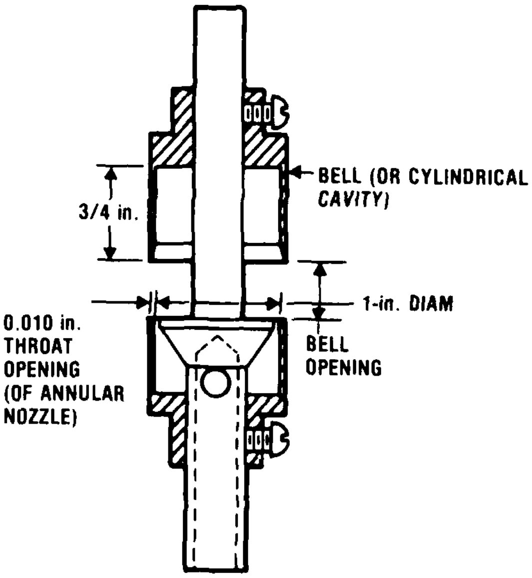

Figure 22. Schematic of Galton whistle (Rice[25]).

TABLE 1. SUMMARY OF JET-FORCING RESONANT-CAVITY COUPLING SYSTEMS STUDIES

[illegible]	[illegible]				[illegible]	[illegible]	[illegible]	[illegible]	[illegible]	[illegible]	[illegible]
	[illegible]	[illegible]	[illegible]	[illegible]							
[illegible][1]	Rectangular	[illegible]	Parallel	No	[illegible]	[illegible]	Fundamental	Yes	[illegible]	Coupling	Yes
[illegible]	Rectangular	[illegible]	Parallel	Yes	[illegible]	[illegible]	Fundamental	Yes	[illegible]	Coupling	Yes
Kirshner (private communication, January 1974)	Rectangular	[illegible]	Parallel	Yes	[illegible]	[illegible]	Fundamental	Yes	[illegible]	Coupling	Yes
[illegible]	[illegible]	[illegible]	[illegible]	Yes	[illegible]	[illegible]	Fundamental	Yes	[illegible]	Coupling	Yes
[illegible]	[illegible]	[illegible]	Normal	Yes	[illegible]	[illegible]	Fundamental	Yes	[illegible]	Coupling	[illegible]
[illegible]	Circular	Circular	Normal	No	--	[illegible]	--	No	--	Coupling	[illegible]
Kimmel and Fischer[?]	Circular	[illegible]	Normal	No	[illegible]	--	[illegible]	Yes	[illegible]	--	[illegible]
[illegible]	[illegible]	[illegible]	[illegible]	No	--	[illegible]	--	Yes	[illegible]	Coupling	[illegible]

[1] [illegible]

[illegible]

5.2 Resonant-Cavity Mechanical-Diaphragm Coupling

The mechanical diaphragm in the fluidic generator is coupled to the cavity by the air volume in the cavity.[9] If the cavity is considered a Helmholtz resonator, then the subsystems are coupled by the fluid capacitor or pneumatic spring, C (see sect. 4.2).

5.3 Mechanical-Diaphragm, Electrical-Circuit/Jet-Forcing Coupling

The diaphragm, connecting rod, and reed assembly are coupled to the electrical circuit by the magnetic transducer circuit shown in figure 15. The magnetic circuit transforms the motion of the reed within the circuit to an ac voltage, which is applied to the electrical circuit. The magnetic circuit is discussed in detail by Leupold et al,[7,8] who developed a computer program to facilitate design optimization of the magnetic circuit of future generators. The computer program lists generator output voltage amplitudes as a function of air gap length (x_a), reed thickness (τ), and reed displacement amplitude (a). The program uses the mathematical procedure of sample calculations given in the report, and it is written in Fortran IV for the Burrough's 5500 computer. Signals reflected from the mechanical diaphragm are fed back to the nozzle exit region of the jet, thereby coupling the mechanical diaphragm and jet-forcing subsystems. This coupling will be discussed further in the following section.

6. PHYSICAL AND MATHEMATICAL MODELS OF FLUIDIC GENERATOR

A cursory physical model describing generator operation was given in the Introduction. In this section, more detailed physical and mathematical models will be given; they are based on the information in sections 4 and 5. Various levels of modeling the generator will be discussed. The fluidic generator will also be analyzed in terms of the input energy supplied to the system.

---

[7] *H. A. Leupold et al, Magnetic Circuit Design Studies for an Inductive Sensor, U.S. Army Electronics Command (ECOM), TR-4158 (October 1973).*

[8] *H. A. Leupold et al, A Flux Circuit Analysis for the Magnetic Transducer of a Fluidic Reed Generator, U.S. Army Electronics Command (ECOM), TR-4284 (January 1975), 2.*

[9] *L. D. Mitchell, Experimental and Theoretical Analysis of a Fluidic Generator, Virginia Polytechnic Institute and State University (in completion of HDL Contract DAAG39-76-R-9164) (August 1977), 4.*

6.1 Physical Model of Fluidic Generator Oscillator Mechanism

The first three subsystems are thought to be interdependent. Moreover, the fluidic generator operating frequency, which is an important aspect of this study, is determined by these subsystems. Therefore, a physical model for this portion of the system will be developed.

The shock wave preceding the fluidic generator inlet in supersonic flight (fig. 3) is stationary relative to the generator (not oscillating) so that the fluid conditions of the air (pressure, temperature, and density) immediately in front of the generator inlet can be determined from normal shock-wave theory. This inlet pressure causes an annular jet (fig. 1) to issue from the annular nozzle and impinge on the annular knife edge of the cavity resonator. In the absence of the cavity (with the knife edge alone), a pressure signal is generated by the impact of the jet against the knife edge. This signal is fed back to the most sensitive region of the jet at the nozzle exit. This disturbance signal at the nozzle exit is amplified by the jet as it is convected forward, toward the knife edge. When the amplified disturbance impacts on the knife edge again, the cycle repeats, and an oscillation is generated. However, in the presence of the cavity (assuming that the diaphragm is rigid), a portion of the jet enters the cavity, and a second pressure signal is generated, which is a function of the cavity's preferred modes or frequencies of oscillation. This signal is also fed back to the nozzle exit region of the jet, where it is amplified by the jet as it is convected in the forward direction toward the cavity. As the jet swings into the cavity, the cycle repeats. The diaphragm is not rigid; therefore, the pressure signal generated in the cavity not only is fed back, but also deflects the diaphragm. The diaphragm has its own preferred modes or frequencies of oscillation; thus, the pressure signal acting on the diaphragm can be amplified or attenuated (cause large or small deflections of the diaphragm), depending on the diaphragm's response characteristics. Thus, a third signal, which is a measure of the characteristic response of the diaphragm, is fed back to the nozzle exit region of the jet where it is amplified as it is convected forward by the jet to complete the cycle.

The combined oscillator system can be described as a Class-III[22] feedback control system (see fig. 23). The jet issuing from the annular nozzle is unstable and has preferred modes of oscillation that are a function of the condition of the inlet ram air (temperature, pressure, and density), and the supply plenum and nozzle geometry. Small disturbances in the supply plenum or nozzle are amplified as they are convected downstream by the jet. This instability, which is independent of downstream obstructions, manifests itself by the oscillation

---

[22] *R. C. Chanaud, Aerodynamic Whistles, Scientific American,* 222, *1 (January 1970), 40 to 46.*

or wavering of the jet. The forward gain in the system is provided by the jet. Pressure feedback signals are generated by sonic reflections from (1) the knife edge, (2) the cavity (assuming that the diaphragm is not moving), and (3) the moving diaphragm. These feedback signals are coupled or summed at the nozzle exit region of the jet to complete the loop. This physical model of the generator, which has been developed in terms of a feedback control system, can be used as the basis for a mathematical model, as discussed in the following section.

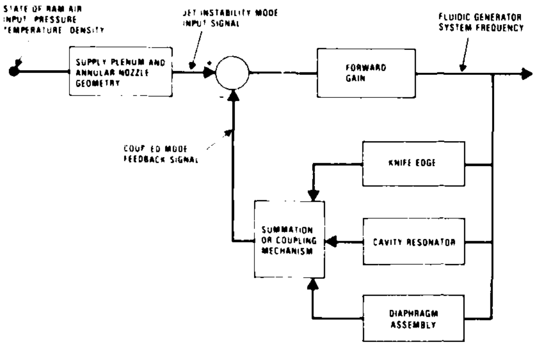

Figure 23. Block diagram of fluidic generator feedback oscillator system.

6.2 Mathematical Model of Fluidic Generator

A mathematical model for the fluidic generator can be developed by using the appropriate mathematical model for the individual subsystems discussed in section 4. However, the following items must be determined experimentally in order to choose the appropriate subsystem model.

(1) The annular jet velocity.
(2) The signal propagation or convection speed in the forward path.
(3) The forward pressure gain of the jet.
(4) The amplitude and path of the feedback signals from the knife edge, the cavity, and the diaphragm.
(5) The speed and coupling of the feedback signals.

The magnetic circuit, which couples the mechanical and electrical subsystems, has a strong loading or damping effect on diaphragm motion. This effect can be modeled with equivalent resistive, inductive, and capacitive impedances--all of which are functions of the

magnetic flux density in the air gap of the magnetic circuit. The computer program by Leupold[8] can be used to determine the magnetic flux density.

The mathematical model of the generator will show the conditions needed for frequency jumps only if the model accounts for the higher harmonic modes of the individual subsystems. It should be noted here that, from the latest MLRS test data, it appears that the fluidic generator operating frequency is primarily influenced by the fundamental oscillating modes of the individual subsystems. However, the generator can be forced into higher modes of oscillation, as described in the next section.

6.3 Generator Input Energy Considerations

The question of jumps in the operating frequency of the fluidic generator is basically an energy consideration. An oscillating system with resonant modes or frequencies will operate at the lowest resonant frequency for which the feedback phase relationships are satisfied, and the system damping is minimal. The fluidic generator is a Class-III[22] oscillating system with acoustic feedback. Therefore, any change in the potential of the input jet will change the signal propagation or convection speed in the forward path and the acoustic speed in the feedback path. This will, in turn, change the feedback phase relationships and can lead to abrupt changes in frequency. The potential energy of the jet changes with changes in generator inlet air pressure and temperature. Therefore, for stable single-mode oscillation, it is necessary to regulate or condition the generator inlet air.

6.4 Computer Simulation

The mathematical model of the generator is needed to (1) determine whether the generator can be forced into unwanted modes of oscillation, (2) optimize generator design, and (3) determine the effect on generator operation caused by parameter changes (parameter changes made to facilitate mass production of the generator). In order to determine the conditions which cause the generator to operate in unwanted modes of oscillation (item (1), sect. 6.2), the generator model must account for higher modes of oscillation of the generator subsystems, as discussed in section 6.2. This undoubtedly will lead to a very complex mathematical model, which must be programmed on the computer for analysis. However, once the range of values for the critical geometric and environmental

---

[8] *H. A. Leupold et al, A Flux Circuit Analysis for the Magnetic Transducer of a Fluidic Reed Generator, U.S. Army Electronics Command (ECOM), TR-4284 (January 1975), 2.*

[22] *R. C. Chanaud, Aerodynamic Whistles, Scientific American, 222, 1 (January 1970), 40 to 46.*

factors have been determined for stable single-mode oscillation, then a less complex model can be used to determine items (2) and (3) above. Thus, time and cost can be saved if part of the computer analysis involves a less complex mathematical model.

Two mathematical models of portions of the fluidic generator have been programmed for use on the computer. They are the computer program of the diaphragm, connecting rod, and reed subsystem model discussed in section 4.3, and the computer program of the magnetic circuit model discussed in section 5.3. Both of these programs will be useful in developing a complete model for the fluidic generator.

7. CONCLUSIONS

The fluidic generator is made up of four subsystems: (1) the jet-forcing mechanism (the annular nozzle and the knife edge of the resonator), (2) the resonant cavity, (3) the mechanical diaphragm assembly (the diaphragm, connecting rod, and reed), and (4) the electrical circuit. The first three subsystems are interdependent and determine the fluidic generator operating frequency. The fluidic generator is a feedback control system in which a steady stream or jet of air is brought into oscillation with a resonant or reflecting structure controlling the feedback. Disturbances, which occur at the nozzle exit, are amplified by the fluid jet and convected downstream. Pressure feedback signals are generated by sonic reflections from (1) the knife edge or shock waves (2) the cavity (assuming that the diaphragm is not moving), and (3) the moving diaphragm. The feedback signals are summed or coupled at the nozzle exit region of the jet. This physical model shows that the generator can be forced to jump to nondesign frequencies of oscillation because any change in the potential of the input jet will change the signal propagation or convection speed in the forward path and the acoustic speed in the feedback path. Thus, the physical model provides a qualitative answer to the question of jumps in the generator operating frequency.

A mathematical model of the complete generator is needed to provide quantitative answers to the question of frequency jumps, to optimize generator designs, and to determine the effect of subsequent parameter changes on generator operation. Such a mathematical model can be developed based on the physical model by synthesizing the appropriate subsystem models. However, in order to determine the appropriate subsystem model, the following generator data must be obtained: the annular jet velocity and pressure gain, the signal propagation speed in the forward and feedback paths, and the amplitude, path, and summation of the feedback signals. Continuing studies on the generator will provide the data needed to develop a mathematical model of the complete generator.

ACKNOWLEDGEMENTS

The author wishes to acknowledge the assistance of H. Lee, M. Salyards, D. Finger, and L. Carlin of Harry Diamond Laboratories for their help in understanding fluidic generator frequency jumps that have occurred in MLRS testing and the corrective measures taken to overcome them. The author also acknowledges the contribution of previously unpublished material by J. Kirshner of HDL and, finally, the assistance of V. Sarohia of the Jet Propulsion Laboratory of the California Institute of Technology in understanding the acoustics and fluid mechanics of generator operation.

LITERATURE CITED

(1) C. J. Campagnuolo, Some Applications of Fluidics in Fuzing, Harry Diamond Laboratories, HDL-TR-1477 (December 1969).

(2) C. J. Campagnuolo, The Fluidic Generator, Harry Diamond Laboratories, HDL-TR-1328 (September 1966).

(3) C. J. Campagnuolo, Fluidic Power Generators for Ordance Application, Harry Diamond Laboratories, HDL-TR-1423 (December 1968).

(4) C. J. Campagnuolo and H. C. Lee, Review of Some Fluid Oscillators, Harry Diamond Laboratories, HDL-TR-1438 (April 1969).

(5) H. S. Kimmel, Development of a Fluidic Velocity Sensor, Harry Diamond Laboratories, HDL-TM-72-6 (March 1972).

(6) H. C. Lee and C. J. Campagnuolo, Development of a High Power Wedge-Type Fluidic Generator, Harry Diamond Laboratories, HDL-TM-72-13 (May 1972).

(7) H. A. Leupold et al, Magnetic Circuit Design Studies for an Inductive Sensor, U.S. Army Electronics Command (ECOM), TR-4158 (October 1973).

(8) H. A. Leupold et al, A Flux Circuit Analysis for the Magnetic Transducer of a Fluidic Reed Generator, U.S. Army Electronics Command (ECOM), TR-4284 (January 1975), 2.

(9) L. D. Mitchell, Experimental and Theoretical Analysis of a Fluidic Generator, Virginia Polytechnic Institute and State University (in completion of HDL Contract DAAG39-76-R-9164) (August 1977), 4.

(10) J. E. Fine, Analysis of Wind Tunnel Test Results of Fluidic Generator for High-Altitude Rocket, HDL-TR-1877 (March 1979).

(11) National Oceanic and Atmospheric Administration, US Standard Atmospheric Tables, Washington, DC (1976).

(12) Ames Research Staff, Equations, Tables, and Charts for Compressible Flow, National Advisory Committee for Aeronautics, Report 1135 (1953).

(13) R. C. Chanaud and A. Powell, Some Experiments Concerning the Hole and Ring Tone, J. Acoust. Soc. Am. 37, 5 (May 1965).

LITERATURE CITED (Cont'd)

(14) G. B. Brown, The Vortex Motion Causing Edgetones, Proceedings of the Physical Society (London), 49 (1937), 493.

(15) A. Powell, On the Edgetone, J. Acoust. Soc. Am., 33, 4 (April 1961), 395 to 409.

(16) V. Sarohia, Some Flight Simulation Experiments on Jet Noise from Supersonic Underexpanded Flows, AIAH Journal, 16, 7 (July 1978), 710 to 716.

(17) A. Powell, On the Mechanism of Choked Jet Noise, Proceedings of the Physical Society, Ser. B, 66 (1956), 1039 to 1056.

(18) R. Sinha, A Theoretical Analysis of Resonance Tube, The Singer Company Kearfott Division, Final Report KD 72-82, for Department of the Army, Picatinny Arsenal, Contract No. DAAA 21-72-C-0500 (October 1972).

(18) A. Powell, On the Mechanism of Choked Jet Noise, Proceedings of the Physical Society, Ser. B, 66 (1956), 1039 to 1056.

(19) A. E. Schmidlin and E. L. Rakowsky, A Jet Driven Flueric Oscillator, Advances in Fluidics, ASME (1967), 282 to 297.

(20) M. E. Franke, G. Jones, III, and H. A. Olsen, Jet Driven Cylindrical Cavity Oscillators, ASME Paper No. 72-WA/Flcs-4 (November 1972).

(21) L. D. Mitchell, Program Documentation: IMPV Class Notes for ME 5120, available from the Department of Mechanical Engineering, Randolph Hall, Virginia Polytechnic Institute and State University, Blacksburg, VA.

(22) R. C. Chanaud, Aerodynamic Whistles, Scientific American, 222, 1 (January 1970), 40 to 46.

(23) W. Gaylord and V. Carter, Flueric Temperature-Sensing Oscillator Design, Harry Diamond Laboratories, HDL-TR-1428 (April 1969).

(24) T. Morel, Experimental Study of a Jet-Driven Helmholtz Oscillator, ASME Winter Annual Meeting, San Francisco, CA (December 1978).

(25) C. W. Rice, Sonic Altimeter for Aircraft, Aeronautical Engineer (Trans. ASME), 4 (1932), 61 to 76.

NOMENCLATURE

a	reed displacement amplitude (m)
A_D	area of diaphragm (m^2)
C_D	electrical equivalent capacitance of the diaphragm (m^5/N)
C_l	electrical capacitance in the generator load circuit (C^2/J)
C_m	electrical equivalent capacitance of a mechanical system (m^5/N)
C_p	electrical equivalent capacitance of a pneumatic system (m^5/N)
c	speed of sound $\sqrt{nP_{avg}/\rho}$, m/s
D_1	diameter of cavity straight section (m)
D_2	diameter of cavity base (m)
f	frequency (Hz)
g	mass rate (kg/s)
j	constant giving edge-tone mode of oscillation (1, 2.3, 3.8, 5.4)
k	mechanical spring of system compliance (N/m)
k_ω	wavelength constant (1/m)
L_D	electrical equivalent inductance of the diaphragm (Ns^2/m^5)
L_C	electrical inductance of the coil in the magnetic circuit (Js^2/C)
L_m	electrical equivalent inductance of mechanical system (Ns^2/m^5)
L_p	electrical equivalent inductance of pneumatic system (Ns^2/m^5)
ℓ	total length of the cavity (m)
ℓ_a	length of the air gap (m)
ℓ_1	length of the cavity straight section (m)
ℓ_2	length of the truncated cone section of the cavity (m)
m	mass of components (kg)
n	polytropic constant
N	constant = 1, 2, 3...
P_{avg}	average pressure in a given volume (N/m^2)
P_1	input pressure at the mouth of the cavity (N/m^2)
P_o	output pressure at the cavity diaphragm (N/m^2)
R_D	electrical equivalent resistance of the diaphragm (Ns/m^5)
R_C	electrical resistance of the coil in the magnetic circuit (ohms)

NOMENCLATURE (Cont'd)

R_m	electrical equivalent resistance of a mechanical system (Ns/m^5)
R_p	electrical equivalent resistance of a pneumatic system (Ns/m^5)
s	Laplace transform variable (1/s)
u	jet velocity at the nozzle (m)
V	cavity volume (m^3)
X	displacement (m)
x	cavity or generator axis (m)
Z_c	electrical impedance of the coil in the magnetic circuit (ohms)
ρ	fluid density (kg/m^3)
ω	angular frequency = $2\pi f$ (rad/s)
τ	reed thickness (m)

DISTRIBUTION

ADMINISTRATOR
DEFENSE DOCUMENTATION CENTER
ATTN DDC-TCA (12 COPIES)
CAMERON STATION, BUILDING 5
ALEXANDRIA, VA 22314

COMMANDER
US ARMY RSCH & STD GP (EUR)
ATTN CHIEF, PHYSICS & MATH BRANCH
FPO NEW YORK 09510

COMMANDER
US ARMY MATERIAL DEVELOPMENT &
READINESS COMMAND
ATTN DRCRD-TP
5001 EISENHOWER AVENUE
ALEXANDRIA, VA 22333

COMMANDER
US ARMY ARMAMENT MATERIEL
READINESS COMMAND
ATTN DRSAR-ASF, FUZE &
MUNITIONS SUPPORT DIV
ATTN DRSAR-RDF, SYS DEV DIV-FUZES
ATTN DRSAR-RDG-T, R. SPENCER
ATTN DRSAR-ASF
ATTN DRSAR-LEP-L, TECH LIBRARY
ROCK ISLAND, IL 61299

COMMANDER
US ARMY MISSILE & MUNITIONS
CENTER & SCHOOL
ATTN ATSK-CTD-F
REDSTONE ARSENAL, AL 35809

DIRECTOR
US ARMY MATERIEL SYSTEMS *ANALYSIS ACTIVITY*
ATTN DRXSY-MP
ABERDEEN PROVING GROUND, MD 21005

DIRECTOR
US ARMY BALLISTIC RESEARCH LABORATORY
ATTN DRDAR-TSB-S (STINFO)
ABERDEEN PROVING GROUND, MD 21005

US ARMY ELECTRONICS TECHNOLOGY
AND DEVICES LABORATORY
ATTN DELET-DD
FORT MONMOUTH, NJ 07703

TELEDYNE BROWN ENGINEERING
CUMMINGS RESEARCH PARK
ATTN MELVIN L. PRICE, MS-44
HUNTSVILLE, AL 35807

HQ USAF/SAMI
WASHINGTON, DC 20330

COMMANDER IDURNE
PENTAGON, ROOM 3D 1089
ATTN G. KOPCSAK
WASHINGTON, DC 20310

OFFICE OF THE DEPUTY CHIEF OF STAFF FOR
RESEARCH, DEVELOPMENT & ACQUISITION
DEPARTMENT OF THE ARMY
ATTN DAMA-ARP-P
ATTN DAMA-CSS
WASHINGTON, DC 20310

US ARMY R&D GROUP (EUROPE)
BOX 15
ATTN CHIEF, AERONAUTICS BRANCH
ATTN CHIEF, ENGINEERING SCIENCES
FPO NEW YORK 09510

US ARMY RESEARCH OFFICE
ATTN R. SINGLETON
P. O. BOX 12211
RESEARCH TRIANGLE PARK, NC 27709

BMD ADVANCED TECHNOLOGY CENTER
ATTN J. PAPADOPOULOS
P. O. BOX 1500
HUNTSVILLE, AL 35807

COMMANDER
US ARMY FOREIGN SCIENCE & TECHNOLOGY CENTER
FEDERAL OFFICE BUILDING
ATTN DRXST-SD1
ATTN DRXST-IS3, C. R. MOORE
220 7TH STREET, NE
CHARLOTTESVILLE, VA 22901

DIRECTOR
APPLIED TECHNOLOGY LABORATORY
ATTN GEORGE W. FOSDICK, DAVDL-ATL-ASA
FORT EUSTIS, VA 23604

COMMANDER
USA MISSILE COMMAND
ATTN REDSTONE SCIENTIFIC INFORMATION
CENTER, *DRSMI-RBD*
ATTN DRDMI-TGC, WILLIAM GRIFFITH
ATTN DRDMI-TGC, J. C. DUNAWAY
ATTN DRCPM-TOE, FRED J. CHEPLEN
REDSTONE ARSENAL, AL 35809

COMMANDER
US ARMY MOBILITY EQUIPMENT R&D CENTER
ATTN TECHNICAL LIBRARY (VAULT)
ATTN DRDME-EM, R. N. WARE
FORT BELVOIR, VA 22060

COMMANDER
EDGEWOOD ARSENAL
ATTN SAREA-MT-T, D. PATTON
ABERDEEN PROVING GROUND, MD 21010

COMMANDER
US ARMY ARRADCOM
ATTN SARPA-TS-S #59
ATTN DRDAR-LCN-C, A. E. SCHMIDLIN
ATTN DRDAR-LCW-E, J. CONNORS
ATTN MICHAEL BACCELLIERI
ATTN PBM-DPM (TAGLAIRINO)
ATTN PBM-MG (A. WILLIAMS)
DOVER, NJ 07801

COMMANDER
WATERVLIET ARSENAL
ATTN SARWV-RDT-L
ATTN DRDAR-LCB-RA, R. RACICOT
WATERVLIET ARSENAL, NY 12189

COMMANDER
US ARMY TANK AUTOMOTIVE RES & DEV COMMAND
ARMOR & COMP DIV, DRDTA-RKT
ATTN T. KOZOWYK
ATTN *A. LAPSYS*
BLDG 215
WARREN, MI 48090

COMMANDER
ATTN STEWS-AD-L, TECHNICAL LIBRARY
WHITE SANDS MISSILE RANGE, NM 88002

COMMANDER/DIRECTOR
ATMOSPHERIC SCIENCES LABORATORY
USA ERADCOM
ATTN *DELAS-AS (HOLT)*
ATTN *DELAS-AS-T (R. RUBIO)*
WHITE SANDS MISSILE RANGE, NM 88002

OFFICE OF NAVAL RESEARCH
DEPARTMENT OF THE NAVY
ATTN STANLEY W. *DOROFF*, CODE 438
ATTN D. S. SIEGEL, CODE 211
ARLINGTON, VA 22217

DEPARTMENT OF THE NAVY
R&D PLANS DIVISION
ROOM 5D760, PENTAGON
ATTN BENJ R. PETRIE, JR.
OP-987P4
WASHINGTON, DC 20350

COMMANDANT
US NAVAL POSTGRADUATE SCHOOL
DEPARTMENT OF MECHANICAL ENGINEERING
ATTN CODE 69 Nn(NUNN)
MONTEREY, CA 93940

COMMANDER
NAVAL AIR DEVELOPMENT CENTER
ATTN R. MCGIBONEY, 30424
ATTN CODE 8134, LOIS GUISE
ATTN D. KEYSER, 30424
WARMINSTER, PA 18974

COMMANDER OFFICER
NAVAL AIR ENGINEERING CENTER
ATTN ESSD, CODE 9314, HAROLD OTT
LAKEHURST, NY 08733

NAVAL AIR SYSTEMS COMMAND
DEPARTMENT OF THE NAVY
ATTN CODE AIR-5162C1, J. BURNS
ATTN CODE AIR-5162C8, D. HOUCK
WASHINGTON, DC 20360

COMMANDER
PACIFIC MISSILE RANGE
NAVAL MISSILE CENTER
ATTN CODE 3123, *ABE J. GARRETT*
ATTN CODE 1243, A. ANDERSON
POINT MUGU, CA 93042

COMMANDER
NAVAL SHIP ENGINEERING CENTER
PHILADELPHIA DIVISION
ATTN CODE 6772
PHILADELPHIA, PA 19112

COMMANDER
NAVAL SURFACE WEAPONS CENTER
ATTN CODE 413, CLAYTON MCKINDRA
ATTN CODE G-4, T. O'CONNOR
WHITE OAK, MD 20910

COMMANDER
NAVAL ORDNANCE STATION
ATTN CODE 5123C, K. ENGLANDER
INDIANHEAD, MD 20640

NAVAL SHIP RES & DEV CENTER
CODE 1619, K. READER
BETHESDA, MD 20084

DISTRIBUTION (Cont'd)

NAVAL SEA SYSTEMS COMMAND
SEA0331H
ATTN A. CHAIKIN
WASHINGTON, DC 20362

COMMANDER
NAVAL WEAPONS CENTER
ATTN CODE 533, LIBRARY DIVISION
ATTN CODE 3636, C. BURMEISTER
CHINA LAKE, CA 93555

COMMANDER
AF AERO PROPULSION LABORATORY, AFSC
ATTN LESTER SMALL, AFWAL/POTC
WRIGHT-PATTERSON AFB, OH 45433

COMMANDER
AIR FORCE AVIONICS LABORATORY
ATTN AARA-2, RICHARD JACOBS
WRIGHT-PATTERSON AFB, OH 45433

DIRECTOR
AF OFFICE OF SCIENTIFIC RESEARCH
ATTN NE, GEORGE KNAUSENBERGER
BOLLING AFB, DC 20332

COMMANDER
AIR FORCE FLIGHT DYNAMICS LABORATORY
ATTN AFFDL/FGL, H. SNOWBALL
ATTN AFFDL/FER, R. J. DOBBEK
WRIGHT-PATTERSON AFB, OH 45433

COMMANDER
AF WEAPONS LABORATORY, AFSC
ATTN SUL, TECHNICAL LIBRARY
KIRTLAND AFB, NM 87117

COMMANDER
ARMAMENT DEVELOPMENT AND TEST CENTER
ATTN ADTC (DLOSL), TECH LIBRARY
ATTN DLMA, DAVID T. WILLIAMS
EGLIN AIR FORCE BASE, FL 32542

AIR FORCE FLIGHT TEST CENTER
6510 ABG/SSD
ATTN TECHNICAL LIBRARY
EDWARDS AFB, CA 93523

AF INSTITUTE OF TECHNOLOGY, AU
ATTN LIBRARY AFIT (LD),
BLDG 640, AREA B
ATTN AFIT (ENM), MILTON E. FRANKE
WRIGHT-PATTERSON AFB, OH 45433

HQ, AF SYSTEMS COMMAND
ATTN SGB, CPT GEORGE JAMES
ANDREWS AFB, DC 20334

OAK RIDGE NATIONAL LABORATORY
CENTRAL RES LIBRARY, BLDG 4500N, RM 175
ATTN E. HOWARD
P. O. BOX X
OAK RIDGE, TN 37830

DEPT OF HEW
PUBLIC HEALTH SERVICE
NATIONAL INSTITUTE OF HEALTH
ATTN C. J. MCCARTHY
BLDG 13, RM 3W-13
BETHESDA, MD 20205

DEPARTMENT OF COMMERCE
NATIONAL BUREAU OF STANDARDS
ATTN JAMES SCHOOLEY, CHIEF,
TEMPERATURE SECTION
ATTN T. NEGAS, SOLID STATE
CHEMISTRY DIVISION
WASHINGTON, DC 20234

DEPARTMENT OF COMMERCE
BUREAU OF EAST-WEST TRADE
OFFICE OF EXPORT ADMINISTRATION
ATTN WALTER J. RUSNACK
WASHINGTON, DC 20230

DEPARTMENT OF JUSTICE
IMMIGRATION AND NATURALIZATION SERVICE
425 "I" STREET NW
ATTN NEILL MCKAY
WASHINGTON, DC 20536

SCIENTIFIC LIBRARY
US PATENT OFFICE
ATTN MRS. CURETON
WASHINGTON, DC 20231

NASA AMES RESEARCH CENTER
ATTN MS 244-13, DEAN CHISEL
MOFFETT FIELD, CA 94035

NASA LANGLEY RESEARCH CENTER
ATTN MS 494, H. D. GARNER
ATTN MS 494, R. R. HELLBAUM
ATTN MS 185, TECHNICAL LIBRARY
HAMPTON, VA 23665

NASA LEWIS RESEARCH CENTER
ATTN VERNON D. GEBBEN
21000 BROOKPARK ROAD
CLEVELAND, OH 44135

NASA SCIENTIFIC & TECH INFO FACILITY
ATTN ACQUISITIONS BRANCH
P. O. BOX 8657
BALTIMORE/WASHINGTON INTERNATIONAL
AIRPORT, MD 21240

UNIVERSITY OF ALABAMA
CIVIL & MINERAL ENGINEERING DEPT.
ATTN HAROLD R. HENRY
P. O. BOX 1468
UNIVERSITY, AL 35486

UNIVERSITY OF ARKANSAS
TECHNOLOGY CAMPUS
ATTN PAUL C. MCLEOD
P. O. BOX 3017
LITTLE ROCK, AR 72203

UNIVERSITY OF ARKANSAS
MECHANICAL ENGINEERING
ATTN JACK H. COLE, ASSOC PROF
FAYETTEVILLE, AR 72701

CARNEGIE-MELLON UNIVERSITY
SCHENLEY PARK
ATTN PROF W. T. ROULEAU, MECH ENGR DEPT
PITTSBURGH, PA 15213

CASE WESTERN RESERVE UNIVERSITY
ATTN PROF P. A. ORNER
ATTN PROF B. HORTON
UNIVERSITY CIRCLE
CLEVELAND, OH 44106

THE CITY COLLEGE OF THE CITY
UNIVERSITY OF NY
DEPT OF MECH ENGR
ATTN PROF L. JIJI
ATTN PROF G. LOWEN
139TH ST. AT CONVENT AVE
NEW YORK, NY 10031

CLEVELAND STATE UNIVERSITY
FENN COLLEGE OF ENGINEERING
ATTN PROF R. COMPARIN
CLEVELAND, OH 44115

DUKE UNIVERSITY
COLLEGE OF ENGINEERING
ATTN C. M. HARMAN
DURHAM, NC 27706

ENGINEERING SOCIETIES LIBRARY
ATTN HOWARD GORDON
ATTN ACQUISITIONS DEPARTMENT
345 EAST 47TH STREET
NEW YORK, NY 10017

FRANKLIN INSTITUTE OF THE STATE
OF PENNSYLVANIA
ATTN KA-CHEUNG TSUI, ELEC ENGR DIV
ATTN C. A. BELSTERLING
20TH STREET & PARKWAY
PHILADELPHIA, PA 19103

HUGHES HELICOPTERS
DIVISION OF SUMMA CORPORATION
CENTINELA & TEALE STREETS
ATTN LIBRARY 2/T2124
CULVER CITY, CA 90230

IIT RESEARCH INSTITUTE
ATTN K. E. MCKEE
10 WEST 35TH STREET
CHICAGO, IL 60616

JOHNS HOPKINS UNIVERSITY
APPLIED PHYSICS LABORATORIES
ATTN MAYNARD HILL
ATTN THOMAS RANKIN
ATTN JOSEPH WALL
LAUREL, MD 20810

LEHIGH UNIVERSITY
DEPARTMENT OF MECHANICAL ENGINEERING
ATTN PROF FORBES T. BROWN
BETHLEHEM, PA 18015

LINDA HALL LIBRARY
ATTN DOCUMENTS DIVISION
5109 CHERRY STREET
KANSAS CITY, MO 64110

MASSACHUSETTS INSTITUTE OF TECHNOLOGY
ATTN ENGINEERING TECHNICAL REPORTS,
RM 10-408
ATTN DAVID WORMLEY, MECH ENGR DEPT,
RM 3-146
77 MASSACHUSETTS AVENUE
CAMBRIDGE, MA 02139

MICHIGAN TECHNOLOGICAL UNIVERSITY
LIBRARY, DOCUMENTS DIVISION
ATTN J. HAWTHORNE
HOUGHTON, MI 49931

DISTRIBUTION (Cont'd)

UNIVERSITY OF MISSISSIPPI
ATTN JOHN A. FOX
201 CARRIER HALL, DEPT OF MECH ENGR
UNIVERSITY, MS 38677

MISSISSIPPI STATE UNIVERSITY
DRAWER ME
ATTN C. J. BELL, MECH ENG DEPT
STATE COLLEGE, MS 39672

UNIVERSITY OF NEBRASKA LIBRARIES
ACQUISITIONS DEPT, SERIALS SECTIONS
ATTN ALAN GOULD
LINCOLN, NE 68508

UNIVERSITY OF NEW HAMPSHIRE
MECH ENGR DEPT, KINGSBURY HALL
ATTN PROF CHARLES TAFT
DURHAM, NH 03824

DEPARTMENT OF MECHANICAL ENGINEERING
NEW JERSEY INSTITUTE OF TECHNOLOGY
ATTN R. Y. CHEN
323 HIGH STREET
NEWARK, NJ 07102

OHIO STATE UNIVERSITY LIBRARIES
SERIAL DIVISION, MAIN LIBRARY
1858 NEIL AVENUE
COLUMBUS, OH 43210

OKLAHOMA STATE UNIVERSITY
SCHOOL OF MECH & AEROSPACE ENGR.
ATTN PROF KARL N. REID
STILLWATER, OK 74074

MIAMI UNIVERSITY
DEPT OF ENG TECH
SCHOOL OF APPLIED SCIENCE
ATTN PROF S. B. FRIEDMAN
OXFORD, OH 45056

PENNSYLVANIA STATE UNIVERSITY
ATTN J. L. SHEARER
215 MECHANICAL ENGINEERING BUILDING
UNIVERSITY PARK, PA 16802

PENNSYLVANIA STATE UNIVERSITY
ENGINEERING LIBRARY
ATTN M. BENNETT, ENGINEERING LIBRARIAN
201 HAMMOND BLDG
UNIVERSITY PARK, PA 16802

PORTLAND STATE UNIVERSITY
DEPT OF ENGINEERING AND
APPLIED SCIENCE
P.O. BOX 751
PORTLAND, OR 97207

PURDUE UNIVERSITY
SCHOOL OF MECHANICAL ENGINEERING
ATTN PROF. VICTOR W. GOLDSCHMIDT
ATTN PROF. ALAN T. MCDONALD
LAFAYETTE, IN 47907

ROCK VALLEY COLLEGE
ATTN KEN BARTON
3301 NORTH MULFORD ROAD
ROCKFORD, IL 61101

RUTGERS UNIVERSITY
LIBRARY OF SCIENCE & MEDICINE
ATTN GOVERMENT DOCUMENTS DEPT
SANDRA R. LIVINGSTON
NEW BRUNSWICK, NJ 08903

SYRACUSE UNIVERSITY
DEPT OF MECH & AEROSPACE ENGINEERING
ATTN PROFESSOR D. S. DOSANJH
139 E. A. LINK HALL
SYRACUSE, NY 13210

UNIVERSITY OF TENNESSEE
DEPT OF MECHANICAL ENGINEERING
ATTN PROF G. V. SMITH
KNOXVILLE, TN 37916

UNIVERSITY OF TEXAS AT AUSTIN
DEPT OF MECHANICAL ENGINEERING
ATTN A. J. HEALEY
AUSTIN, TX 78712

THE UNIVERSITY OF TEXAS AT ARLINGTON
MECHANICAL ENGINEERING DEPARTMENT
ATTN ROBERT L. WOODS
ARLINGTON, TX 76019

TULANE UNIVERSITY
DEPT OF MECHANICAL ENGINEERING
ATTN H. F. HRUBECKY
NEW ORLEANS, LA 70118

UNION COLLEGE
MECHANICAL ENGINEERING
ATTN ASSOC PROF W. C. AUBREY
MECH ENGR DEPT, STEINMETZ HALL
SCHENECTADY, NY 12308

VIRGINIA POLYTECHNIC INSTITUTE OF STATE UNIV
MECHANICAL ENGINEERING DEPARTMENT
ATTN PROF H. MOSES
BLACKSBURG, VA 24061

WASHINGTON UNIVERSITY
SCHOOL OF ENGINEERING
ATTN W. M. SWANSON
P. O. BOX 1185
ST. LOUIS, MO 63130

WEST VIRGINIA UNIVERSITY
MECHANICAL ENGINEERING DEPARTMENT
ATTN RICHARD A. BAJURA
MORGANTOWN, WV 26505

WICHITA STATE UNIVERSITY
ATTN DEPT AERO ENGR, E. J. RODGERS
WICHITA, KS 67208

UNIVERSITY OF WISCONSIN
MECHANICAL ENGINEERING DEPARTMENT
ATTN FEDERAL REPORTS CENTER
ATTN NORMAN H. BEACHLEY, DIR,
DESIGN ENGINEERING LABORATORIES
1513 UNIVERSITY AVENUE
MADISON, WI 53706

WORCESTER POLYTECHNIC INSTITUTE
ATTN GEORGE C. GORDON LIBRARY (TR)
ATTN TECHNICAL REPORTS
WORCESTER, MA 01609

AIRESEARCH
P. O. BOX 5217
ATTN GARY FREDERICK
ATTN TREVOR SUTTON
ATTN TOM TIPPETTS
111 SOUTH 34TH STREET
PHOENIX, AZ 85010

AVCO SYSTEMS DIVISION
ATTN W. K. CLARK
ATTN R. LIMPAECHER
201 LOWELL STREET
WILMINGTON, MA 01887

BELL HELICOPTER COMPANY
ATTN R. D. YEARY
P. O. BOX 482
FORTWORTH, TX 76101

BENDIX CORPORATION
ELECTRODYNAMICS DIVISION
ATTN D. COOPER
11600 SHERMAN WAY
N. HOLLYWOOD, CA 90605

BENDIX CORPORATION
RESEARCH LABORATORIES DIV.
BENDIX CENTER
ATTN C. J. AHERN
SOUTHFIELD, MI 48075

BOEING COMPANY, THE
ATTN HENRIK STRAUB
P. O. BOX 3707
SEATTLE, WA 98124

BOWLES FLUIDICS CORPORATION
ATTN VICE PRES./ENGR.
9347 FRASER AVENUE
SILVER SPRINGS, MD 20910

RONALD BOWLES
2105 SONDRA COURT
SILVER SPRING, MD 20904

CHAMBERLAIN MANUFACTURING CORP
ATTN W. J. WESTERMAN
EAST 4TH AND ESTHER STS
P.O. BOX 2545
WATERLOO, IA 50705

CONTINENTAL CAN COMPANY
TECH CENTER
ATTN P. A. BAUER
1350 W. 76TH STREET
CHICAGO, IL 60620

CORDIS CORPORATION
ATTN STEPHEN F. VADAS, K-2
P. O. BOX 428
MIAMI, FL 33137

CORNING GLASS WORKS
FLUIDIC PRODUCTS
ATTN R. H. BELLMAN
HOUGHTON PARK, B-2
CORNING, NY 14830

CHRYSLER CORPORATION
P. O. BOX 118
CIMS-418-33-22
ATTN L. GAO
DETROIT, MI 48231

DISTRIBUTION (Cont'd)

JOHN DEERE PRODUCT ENGINEERING CENTER
ATTN V. S. KUMAR
WATERLOO, IA 50704

ELECTRIC POWER RESEARCH INSTITUTE
3412 HILLVIEW AVE
P.O. BOX 10412
ATTN MS. M. ANGWIN,
P. M. GEOTHERMAL ENERGY
PALO ALTO, CA 94303

FLUIDICS QUARTERLY
ATTN D. H. TARUMOTO
P. O. BOX 2989
STANFORD, CA 94305

GENERAL ELECTRIC COMPANY
SPACE/RESD DIVISIONS
ATTN MGR LIBRARIES, LARRY CHASEN
P. O. BOX 8555
PHILADELPHIA, PA 19101

GENERAL ELECTRIC COMPANY
KNOLLS ATOMIC POWER LABORATORY
ATTN D. KROMMENHOEK
SCHENECTADY, NY 12301

GENERAL MOTORS CORPORATION
DELCO ELECTRONICS DIV
MANFRED G. WRIGHT
NEW COMMERCIAL PRODUCTS
ATTN R. E. SPARKS
P. O. BOX 1104
KOKOMO, IN 46901

GRUMMAN AEROSPACE CORPORATION
TECHNICAL INFORMATION CENTER
ATTN C. W. TURNER, DOCUMENTS
LIBRARIAN
SOUTH OYSTER BAY ROAD
BETHPAGE, L. I., NY 11714

HAMILTON STANDARD
DIVISION OF UNITED AIRCRAFT CORPORATION
ATTN PHILIP BARNES
WINDSOR LOCKS, CT 06096

HONEYWELL, INC
ATTN J. HEDEEN
1625 ZARTHAN AVE
MINNEAPOLIS, MN 55413

JOHNSON CONTROLS, INC
ATTN WARREN A. LEDERMAN
ATTN GEORGE JANU
507 E MICHIGAN
MILWAUKEE, WI 53201

MOORE PRODUCTS COMPANY
ATTN R. ADAMS
SPRING HOUSE, PA 19477

MARTIN MARIETTA CORPORATION
AEROSPACE DIVISION
ATTN R. K. BRODERSON, MP 326
P. O. BOX 5837
ORLANDO, FL 32805

MCDONNELL AIRCRAFT COMPANY
GUIDANCE AND CONTROL MECHANICS DIVISION
ATTN LOYAL GUENTHER
ST. LOUIS, MO 63166

MCDONNELL DOUGLAS ASTRONAUTICS CO
PROPULSION DEPARTMENT
ATTN V. E. HALOULAKOS (A3-226)
ATTN J. D. SCHWEIKLE (A3-226)
5301 BOLSA AVENUE
HUNTINGTON BEACH, CA 92647

NATIONAL FLUID POWER ASSOCIATION
ATTN JOHN R. LUEKE
DIR OF TECH SERVICES
3333 NORTH MAYFAIR ROAD
MILWAUKEE, WI 53222

NEOS, INC
3711 AIR PARK RD
ATTN A. J. OSTDIEK
LINCOLN, NE 68524

PLESSEY AEROSPACE LTD
ATTN A. ROSENBERG
1700 OLD MEADOW ROAD
MCLEAN, VA 22102

RICHARD WHITE & ASSOCIATES
ELECTRO/MECHANICAL ENGINEERS
ATTN RICHARD P. WHITE
77 PELHAM ISLE ROAD
SUDSBURY, MA 01776

ROCKWELL INTERNATIONAL CORPORATION
COLUMBUS AIRCRAFT DIVISION, P. O. BOX 1259
ATTN MARVIN SCHWEIGER
4300 E 5TH AVENUE
COLUMBUS, OH 43216

SANDIA LABORATORIES
ATTN WILLIAM R. LEUENBERGER, DIV 2323
ATTN JERRY HOOD
ATTN NED KELTNER
ALBUQUERQUE, NM 87185

SCIENCE APPLICATIONS, INC
8400 WESTPARK DR
ATTN J. ISEMAN
MCLEAN, VA 22102

SIKORSKY AIRCRAFT
NORTH MAIN STREET
ATTN J. R. SOEHNLEIN
STRATFORD, CT 06602

STEIN ENGINEERING SERVICES, INC
5602 E. MONTEROSA
PHOENIX, AZ 85018

TRANS-TECH, INC
12 MEEM AVE
ATTN L. DOMINGUES
GAITHERSBURG, MD 20760

TRITEC, INC
ATTN L. SIERACKI
P. O. BOX 56
COLUMBIA, MD 21045

UNITED TECHNOLOGIES RESEARCH CENTER
ATTN R. E. OLSON, MGR FLUID
DYNAMICS LABORATORY
400 MAIN STREET
E. HARTFORD, CT 06108

WESTINGHOUSE ELECTRIC CORP
1310 BEULAH RD
ATTN F. GOLDSCHMEID
PITTSBURGH, PA 15235

US ARMY ELECTRONICS RESEARCH
& DEVELOPMENT COMMAND
ATTN TECHNICAL DIRECTOR, DRDEL-CT

HARRY DIAMOND LABORATORIES
ATTN 00100, CO/TD/TSO/DIV DIRS
ATTN RECORD COPY, 81200
ATTN HDL LIBRARY, (3 COPIES), 81100
ATTN HDL LIBRARY, (WOODBRIDGE), 81100
ATTN TECHNICAL REPORTS BRANCH, 81300
ATTN CHAIRMAN, EDITORIAL COMMITTEE
ATTN CORRIGAN, J., 20240
ATTN CHIEF, 13000
ATTN CHIEF, 13400 (10 COPIES)
ATTN LANHAM, C., 00210 (3 COPIES)
ATTN DEADWYLER, R., 13400 (10 COPIES)
ATTN GOODMAN, R., 34400
ATTN FEMENIAS, R., 22100